

Influencers identification in complex networks through reaction-diffusion dynamics

Flavio Iannelli,¹ Manuel S. Mariani,^{2,3,4} and Igor M. Sokolov¹

¹*Institute for Physics, Humboldt-University of Berlin, Newtonstraße 15, 12489 Berlin, Germany **

²*Institute of Fundamental and Frontier Sciences, University of Electronic Science and Technology of China, Chengdu 610054, PR China*

³*URPP Social Networks, Universität Zürich, 8050 Zürich, Switzerland*

⁴*Department of Physics, University of Fribourg, 1700 Fribourg, Switzerland*

(Dated: March 17, 2022)

A pivotal idea in network science, marketing research and innovation diffusion theories is that a small group of nodes – called influencers – have the largest impact on social contagion and epidemic processes in networks. Despite the long-standing interest in the influencers identification problem in socio-economic and biological networks, there is not yet agreement on which is the best identification strategy. State-of-the-art strategies are typically based either on heuristic centrality metrics or on analytic arguments that only hold for specific network topologies or peculiar dynamical regimes. Here, we leverage the recently introduced random-walk effective distance – a topological metric that estimates almost perfectly the arrival time of diffusive spreading processes on networks – to introduce a new centrality metric which quantifies how close a node is to the other nodes. We show that the new centrality metric significantly outperforms state-of-the-art metrics in detecting the influencers for global contagion processes. Our findings reveal the essential role of the network effective distance for the influencers identification and lead us closer to the optimal solution of the problem.

Networks constitute the substrate for the spreading of agents as diverse as opinions [1, 2], rumors [3], computer viruses [4], and deadly pathogens [5]. Differently from classical epidemiological [6] and collective behavior models [7], which typically assume homogeneously mixed populations, the network approach assumes that agents can only spread through the links of an underlying network of contacts [5]. Network-mediated spreading processes are ubiquitous: for example, online users transmit news and information to their contacts in online social platforms [8–10]; individuals form their opinion and make decisions influenced by their contacts in social networks [1, 2, 11]; infected individuals can transmit infectious diseases to their sexual partners [12].

A long-standing idea in network science, marketing research and innovation diffusion theories is that in a given network, a tiny set of nodes – called *influencers* – have the largest impact on social contagion and epidemic spreading processes. Many studies have aimed to accurately identify [13–15], target [16, 17], and assess the impact of [18, 19] the influencers for marketing purposes. Proper identification and targeting are vital for organizations to design effective marketing campaigns in order to maximize their chances of success [13, 20, 21], for policy-makers to design effective immunization strategies against infectious diseases [22], for social media companies to maximize the outreach of a given piece of information, such as a news or a meme [23].

The influencers identification problem is typically studied by using epidemic spreading and social contagion models to simulate multiple independent realizations of spreading processes on real networks. Different processes

are initiated by different “seed” nodes; the typical size of the outbreak generated by a given node quantifies its “ground-truth” spreading ability [15, 24–27]. One can thus compare different node ranking algorithms with respect to their ability to identify the nodes with the largest ground-truth spreading ability [15, 24]. The seminal work by Kitsak et al. [24] showed that the nodes with the largest number of contacts (“hubs” in the network science literature [28]) are not necessarily the most influential spreaders, and nodes with fewer connections but located in strategic network positions can initiate larger spreading processes. Following Kitsak et al. [24], several network centrality metrics [15, 29] – originally aimed at quantifying individuals’ influence and prestige in social networks [30] – have been compared with respect to their ability to identify the influential spreaders [23, 25–27, 31–36]. The results of this massive effort have been often contradictory, and there is not yet agreement on which is the best metric for the influencers identification.

The current lack of agreement on which metric best quantifies the spreading ability of the nodes can be ascribed to two main limitations of existing studies. First, most of the proposed centrality metrics do not consider the properties of the spreading dynamics in exam [24, 31, 34, 37], or they are based on analytic arguments that are valid only for specific types of networks and spreading parameters [27]. As a result, the performance of these metrics strongly depends on network topology and on the parameters that rule the target epidemic process. Second, existing works often restrict the comparison of the metrics’ performance to a limited number of parameter values [15, 27], which leaves it unclear how the relative performance of the metrics depends on model parameters.

In this article, we overcome both limitations. We in-

* iannelli.flavio@gmail.com

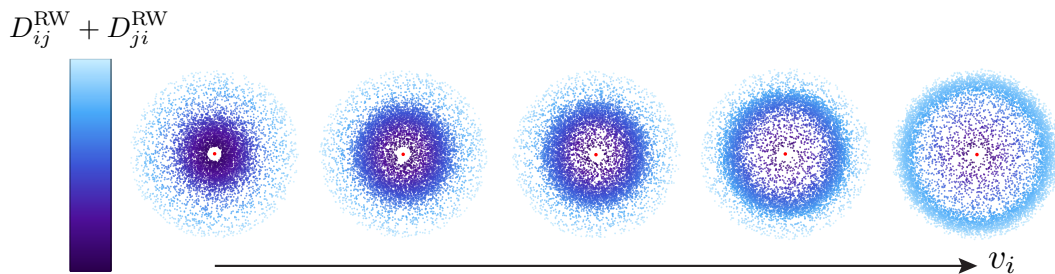


FIG. 1. Illustration of the ViralRank centrality in terms of the random-walk effective distance D_{ij}^{RW} for different seed nodes i (the central red circles in the figure). The clouds of nodes around each seed node i represent the other nodes $\{j\}$ in the network. Their radial distance from the center of the cloud is proportional to their total random-walk effective distance ($D_{ij}^{RW} + D_{ji}^{RW}$) from the source node i ; their color ranges from dark-blue (low distance) to white (high distance). The average effective distance yields the ViralRank score $v_i(\lambda)$ (horizontal axis). The cases depicted here evolve continuously from a central node (small v_i , left side of the panel) which tends to be close to many other nodes, to a peripheral seed node (large v_i , right side of the panel) which tends to be far from the other nodes.

introduce a new centrality metric, which we call *ViralRank*, directly built on the random-walk effective distance for reaction-diffusion spreading processes [38]. In particular, the ViralRank score of a node is defined as its average random-walk effective distance to and from all the other nodes in the network. The rationale behind this definition is that an influential spreader should be able to reach and to be reached quickly from the other nodes. As the random-walk effective distance quantifies almost perfectly the infection arrival time for any source and target node in reaction-diffusion processes [38], we expect the average effective distance to accurately quantify how well a node can reach and be reached by the other nodes.

Our results show that ViralRank is the most effective metric in identifying the influential spreaders for global contagion processes – both contact-network processes in the supercritical regime, and reaction-diffusion spreading processes. In contact networks, if the disease transmission probability is sufficiently large, ViralRank is systematically the best metric to quantify the spreading ability of a node. We provide evidence that – differently from what was previously stated [24, 27] – values of the transmission probability well above the critical point are relevant values to real spreading processes. In the metapopulation model, ViralRank is the best-performing metric for almost all the analyzed parameter values. Besides, we show analytically that ViralRank can be written in terms of the classical Friedkin-Johnsen social influence model, introduced in [2] and recently used to predict individuals' final opinions in controlled experiments [11, 39]. We also show that the Google's PageRank [40] score can be re-interpreted as the average of a specific *partition function* built on the network effective distance.

Our findings demonstrate that the effective distance between pairs of nodes can be used to quantify the nodes' spreading ability significantly better than with existing metrics, bringing us closer to the optimal solution to the problem of identifying the influential spreaders for both

contact-network and reaction-diffusion processes.

RESULTS

We start by defining the new metric (ViralRank) and then validate it as a metric for the influential spreaders identification for contact-network and reaction-diffusion processes. *Contact-network* models of spreading assume that individuals directly "infect" the individuals they are in contact with. Crucially, the topology of the underlying network of contacts plays a critical role in determining the size of the infected population [42, 43]. On the other hand, to describe global contagion processes, *reaction-diffusion* models assume that individuals can infect the individuals that belong to the same population (reaction process) and in addition, infected individuals can move across populations (diffusion process).

Effective distance and ViralRank

Previous works [38, 44] have pointed out that in order to predict the hitting time of a spreading process in geographically-embedded systems, network topology and the corresponding weight flows play a more fundamental role than the geographical distance. The main idea behind ViralRank is to rank the nodes based on the random-walk effective distance $D_{ij}^{RW}(\lambda)$ between pairs of nodes which quantifies almost perfectly the hitting time of a reaction-diffusion spreading process on the network [38]. Importantly, the calculation of $D_{ij}^{RW}(\lambda)$ only requires the network adjacency matrix $\{A_{ij}\}$ as input, whereas λ is a parameter that depends on the spreading dynamics (see below).

We define the ViralRank score of a node i as the average random-walk effective distance from all sources and

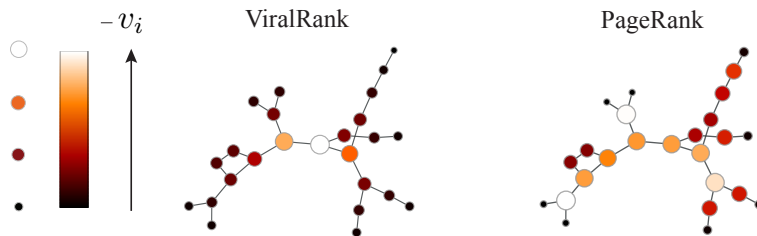


FIG. 2. A comparison between ViralRank and PageRank for a toy small-world undirected network with $N = 25$ nodes. In line with [41], the network is built by starting from a ring topology where each node has 5 neighbors, and by rewiring each edge with probability $p = 0.5$. The size of each node is proportional to the value of the corresponding score normalized by the maximum score in the network, and the color scale changes accordingly.

to all target nodes in the network [45]

$$v_i(\lambda) = \frac{1}{N} \sum_j (D_{ij}^{\text{RW}}(\lambda) + D_{ji}^{\text{RW}}(\lambda)), \quad (1)$$

where the effective distance is defined by [38]

$$D_{ij}^{\text{RW}}(\lambda) = -\ln \left(\sum_{k \neq j} \left(\mathbf{I}^{(j)} - e^{-\lambda} \mathbf{P}^{(j)} \right)_{ik}^{-1} e^{-\lambda} p_k^{(j)} \right) \quad (2)$$

for $i \neq j$, whereas $D_{ii}^{\text{RW}}(\lambda) = 0$. The argument of the logarithm is a function that counts all the random-walks that start in i and end when arriving in j – we refer to it as *partition function*, see Appendix B. Here, $\mathbf{P}^{(j)}$ and $\mathbf{I}^{(j)}$ are the $(N-1) \times (N-1)$ submatrices of the Markov matrix $(\mathbf{P})_{ij} = A_{ij} / \sum_k A_{ik}$ and of the identity matrix $(\mathbf{I})_{ij} = \delta_{ij}$, respectively, obtained by excluding the j th row and j th column; $\mathbf{p}^{(j)}$ is the j th column of \mathbf{P} after removing the j th component. The nodes are therefore ranked in order of *increasing* ViralRank score: a node is central if it has, on average, small effective distance from and to the other nodes in the network [46]. As the nodes ranked high by ViralRank tend to have small effective distance from the other nodes, we expect them to generate larger epidemic outbreaks than peripheral nodes when they are chosen as the “seed” nodes of a spreading process (see Fig. 1). Testing the validity of this hypothesis is one of the main goals of this paper.

For reaction-diffusion spreading processes based on a metapopulation model, the interpretation of $D_{ij}^{\text{RW}}(\lambda)$ as a proxy for the hitting time of the spreading process makes the parameter λ unambiguously determined by the parameters of the reaction dynamics of interest (see [38]). For contact-network spreading processes, a clear-cut criterion to choose λ is lacking. Our analytic results (see Appendix B) show that in the limit $\lambda \rightarrow 0$, the ViralRank score of a given node i reduces to the average mean first-passage time (MFPT) needed for a random walk starting in node i to reach the other nodes, plus the MFPT [47] needed for a random walk starting in the nodes other than i to reach node i . In the following, for contact-network spreading, we therefore consider the quantity $v_i = v_i(\lambda \rightarrow 0)$ as node i ’s ViralRank score. With this

choice, a node i is central if a random walk starting at node i is able to quickly reach the other nodes in the network and, at the same time, it is well reachable from all other nodes.

In Appendices C and D, we show that (1) there is a mathematical relation between ViralRank and the Friedkin-Johnsen (FJ) opinion formation model; (2) Google’s PageRank can be also expressed, as ViralRank, in terms of a specific partition function. Our analytic computations reveal the two main differences between ViralRank and PageRank: (1) differently from the ViralRank score, the PageRank score does not depend logarithmically on its partition function, but linearly. This means that if a seed node i is far from a node j in the network, this will result in a small positive contribution to node i ’s PageRank score; by contrast, it will result in a large contribution (penalization) to its ViralRank score, proportional to D_{ij}^{RW} . (2) The specific partition function used by PageRank also includes the walks that hit several times the arrival nodes, which results in a poor estimate of the diffusion hitting time.

These two factors impair PageRank’s ability to identify central nodes in networks. We show this by analyzing a toy small-world Watts-Strogatz [41] network with a clear distinction between central and peripheral nodes, see Fig. 2. The standard PageRank with damping parameter [48] equal to 0.85 gives a comparable score to peripheral nodes, located at the end of a branch, and central nodes, whereas ViralRank is able to clearly identify central nodes. In Figure S3, we show that PageRank is always outperformed by the degree centrality in the influential spreaders identification; for this reason, we do not show its performance here.

Influential spreaders identification: Results for contact networks

After having defined ViralRank and discussed its relation with PageRank and the FJ opinion formation model, we validate it as a metric for the influential spreaders identification. The metrics considered here for comparison are the following: degree k (or strength s for weighted

Network	N	L	D	C	$\langle k \rangle$	β_u/β_c
Terrorists	62	152	5	0.49	4.90	2.50
Email	167	3250	5	0.59	38.92	6.50
Jazz	198	2742	6	0.62	27.70	4.25
NetScientists	379	914	17	0.74	1.15	2.00
Protein	1458	1948	19	0.07	2.08	2.25
Facebook	4039	88234	8	0.61	43.69	4.75

TABLE I. Structural properties of the analyzed empirical networks: the different quantities represent the number of nodes (N) and links (L), the diameter (D), the clustering coefficient (C), the first ($\langle k \rangle$) moment of the degree distribution, and the upper-critical threshold (β_u) above which ViralRank outperforms all the other metrics, as a multiple of the SIR epidemic threshold β_c .

networks), k-core centrality k_c [24], random-walk accessibility (RWA) [25], LocalRank (LR) [31] and the non-backtracking centrality (NBC) [49]. All these metrics are defined in Supplementary Note S1.

Spreading dynamics. In this section, we consider *contact-network* spreading processes where the spreading agent is directly transmitted from an infected node to its susceptible neighbors. More specifically, we consider a susceptible-infected-removed (SIR) model, which is one of the most studied mathematical models for epidemic spreading processes on networks. At each time step, each individual (node) can be in one of three states: susceptible, infected, or removed. At each time step, each infected node can infect each of its neighbors with probability β , and infected individuals are removed from the dynamics with probability μ . The epidemic spreading process terminates when there is no infected node in the network and the disease cannot propagate anymore. To assess the metrics' performance in the influential spreaders identification, we compare the score they produce with the score of the nodes by their spreading ability [15, 24]. The spreading ability q_i of node i is defined as the average number of nodes in the removed state after the infection process has ended, given that the process was initiated by node i – i.e., node i was the only infected node at time $t = 0$. For each node i , this average is based on 10^3 independent realizations of the stochastic SIR dynamics described above.

For the SIR model, there exists a critical value (referred to as epidemic threshold [50]) $\beta = \beta_c$ such that the spreading process, once initiated, quickly dies out for $\beta < \beta_c$, whereas it infects a significant portion of the network for $\beta > \beta_c$. We expect the distance of β from β_c to significantly affect the relative metrics' performance, an aspect that is typically not extensively investigated in existing works on the influential spreaders identification. Below, we study how the metrics' performance depends on β/β_c .

Results. We analyze six empirical networks (see Table I for a summary of their properties) in which we simulate the SIR spreading process: (a) 9/11 terrorists, (b) emails, (c) jazz collaborations, (d) network scientists co-

authorships, (e) protein interactions and (f) Facebook friendships. The meaning of the nodes and the links in the datasets and the datasets' properties are explained in Appendix A. The results for six additional empirical datasets are shown in Fig. S4 and are in qualitative agreement with the results shown here.

We find (Fig. S4) that for all the analyzed datasets, there exists a dataset-dependent value β_u such that ViralRank is the best-performing metric for $\beta > \beta_u$. The value β_u is always larger than β_c , which confirms that ViralRank is the most effective metric for the identification of influential spreaders for spreading processes in the supercritical regime. The largest ($\beta_u = 6.5 \beta_c$) and smallest ($\beta_u = 2 \beta_c$) values of β_u are observed for the email and the scientists co-authorships, respectively. By contrast, other metrics perform better in the vicinity of the critical point; which metric performs best in this parameter region critically depends on the considered dataset. At the critical point β_c , the best performing metrics are, for almost all datasets, the NBC and LR. Interestingly, for all the analyzed datasets, k_c is the second-best performing metric (after ViralRank) in the supercritical regime.

These results demonstrate that among the existing metrics, there is no universally best-performing metric; the only consistent conclusion is that ViralRank outperforms all the other metrics for processes sufficiently far from criticality. Therefore, the optimal choice of a metric for identifying the influential spreaders critically depends not only on the considered dataset but also on the parameters of the particular spreading process. Remarkably, in most of the analyzed datasets, not only ViralRank outperforms other metrics in the $\beta > \beta_u$ range, but it also approaches the perfect correlation with the spreading ability, $r(-v, q) \simeq 1$, for specific ranges of β values within the supercritical region.

Results on synthetic networks confirm the existence of $\beta_u > \beta_c$. Besides, by gradually perturbing a scale-free network, we are able to gradually move from a scale-free to a Poissonian topology (see Supplementary Note S2 for details). The results on thus-generated synthetic networks show that differently from existing metrics' performance, ViralRank's performance is little sensitive to the network degree distribution (Fig. S1).

In the model-based setting adopted here (borrowed from the epidemiology and network science literature [15, 24]), the propagation of real diseases and computer viruses falls in the supercritical regime, and often in the parameter region where ViralRank is the best performing metric in identifying the influential spreaders (see Supplementary Fig. S2). Besides, the supercritical region is also the most relevant from a marketing point of view: if the dynamics parameters force most of the spreading processes to die out quickly, it becomes virtually impossible for an influencer to initiate large-scale adoption cascades [18]. A study of the problem in a more realistic setting goes beyond the scope of this work as it would require a more complex model of propagation, an accurate calibration of model parameters, and the possibility

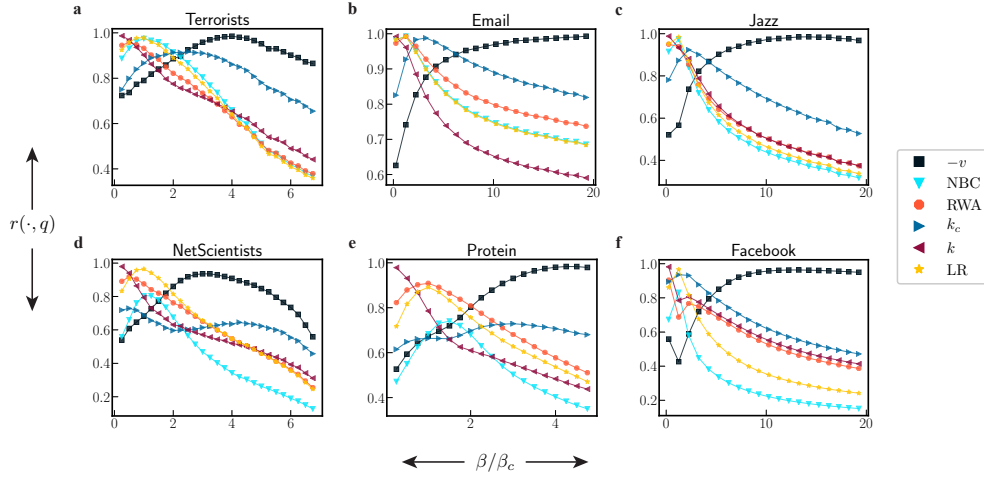


FIG. 3. Contact-network spreading model: a comparison between nodes' centrality and nodes' spreading ability q in real networks. Pearson's linear correlation between nodes' centrality and q as a function of β/β_c for the datasets described in Table I.

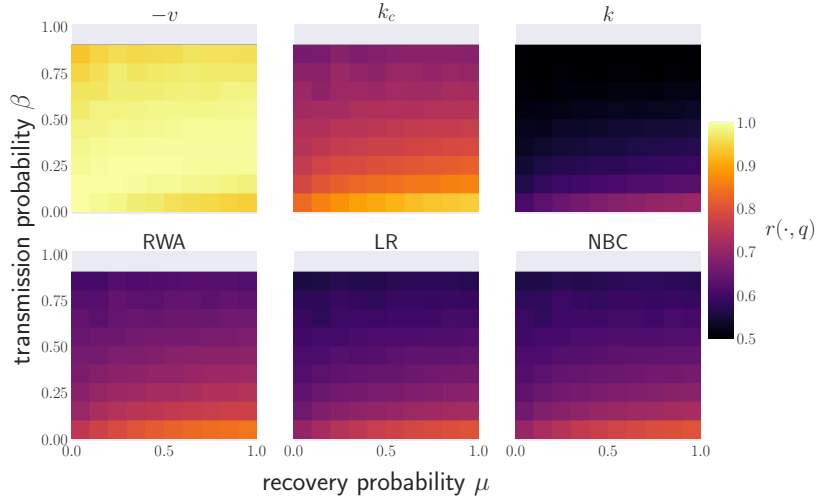


FIG. 4. Contact-network spreading model: a comparison between node centrality and node spreading ability q in the whole parameter space, for the email network ($\beta_c = 0.0158\mu$) – results for the other analyzed datasets are reported in the Supplementary Figures S5-S9. The heatmap represents the Pearson's correlation coefficient $r(\cdot, q)$ between the nodes' centrality score and spreading ability in the (β, μ) parameter space; the colors range from black ($r = 0.5$) to yellow ($r = 1$).

of external intervention (such as vaccination and travel restriction in the case of diseases).

While ViralRank consistently outperforms the other metrics for $\beta > \beta_u$, we expect its performance to dwindle as β approaches one. Indeed, for $\beta = 1$, all the network nodes are eventually in the recovered state for any starting node and, as a result, the nodes all have spreading ability equal to one. To quantify the extent of the parameter region over which we are able to quantify the nodes' spreading ability, we study the complete parameter space (β, μ) of transmission and recovery probability. We find (Figs. 4 and S5-S9) that ViralRank is able to quantify the spreading ability, for a much larger parameter region than existing metrics. Remarkably, for the emails net-

work (Fig. 4), the correlation between ViralRank and the spreading ability q is still larger than 0.95 for values of β as large as $\beta = 0.9$ and still larger than 0.90 even for $\beta = 0.99$. By contrast, for such large values of β , all the other metrics are essentially uncorrelated with q . Only at the saturation value $\beta = 1$ ViralRank loses its correlation with nodes' spreading ability.

Influential spreaders identification: Results for reaction-diffusion spreading processes

Reaction-diffusion dynamics. While contact-network spreading processes can model the spreading of an infec-

tion within a networked population, in order to properly model global contagion processes, we need to take into account that multiple individuals, of different epidemiological compartments, can only interact with individuals that are located in the same geographical location. This realization has motivated the study of metapopulation models, where each node represents a geographical location, and it is occupied by a subpopulation composed of a subset of all the individuals. At each time step of the dynamics, individuals can (1) interact with individuals located at the same node (*reaction*); (2) travel across locations (*diffusion*). Reaction-diffusion models of spreading are increasingly used to forecast the properties of epidemic outbreaks [51–53], and to design and understand the systemic impact of disease containment strategies [52, 54].

In the following, in line with previous studies [38, 44], we assume that the reaction dynamics is ruled by the fully-mixed SIR model; the generalization to arbitrary compartment models is obviously possible, but the SIR model often provides the sufficient level complexity necessary to describe real epidemic processes [55]. We study epidemics spreading through the U.S. air transportation network (see Appendix A for details on the data): each node j represents an airport and it is occupied by a subpopulation of size N_j ; each airport is connected to the others via the weighted adjacency matrix W_{ij} . The weight W_{ij} represents the undirected flux of passengers between airport i and j as observed in the data. The probability that an individual located at node i will travel to node j at a given time is proportional to the transition matrix element $P_{ij} = W_{ij} / \sum_k W_{ik}$ (see Supplementary Note S2 for details on the model).

Identification of influential spreader populations. Despite the growing interest in reaction-diffusion processes [44, 51, 55, 56], also spurred by their application to disease forecasting [53], the identification of influential spreaders for such dynamics has attracted less attention compared to the analogous problem for contact-network spreading processes. Here, we fill this gap by comparing different centrality metrics with respect to their ability to identify those airports that are able to infect a large portion of the network in a relatively short time.

To simulate the spreading process, we numerically integrate the set of deterministic non-linear differential equations that describe the SIR reaction-diffusion process with non-stochastic transport (see Supplementary Note S2 for details). In the metapopulation model, a non-trivial dynamics is obtained only above the critical threshold, where all nodes will eventually contain at least one infected individual after a sufficiently long time. This, however, makes it impossible to quantify the nodes’ ground-truth spreading ability by measuring the asymptotic number of nodes with at least one infected individual. To avoid this, we halt the simulations at a given threshold time $t_{max}(R_0) = (2R_0\alpha)^{-1}$, where $R_0 = \beta/\mu$ and α are the basic reproductive number and diffusion rate, respectively (see Supplementary Note S2 for the

details). We then quantify nodes’ spreading ability as the fraction of populations $\omega(t_{max})$ that contain at least one infected individual at time t_{max} . The performance of a metric is quantified by the correlation between the scores it produces and $\omega(t_{max})$ – we refer to $\omega(t_{max})$ as the *prevalence*.

Results. We compare the performance of all the previously considered centrality metrics, by replacing the unweighted degree centrality with the strength $s_i = \sum_j W_{ij}$. We find that the ViralRank centrality $v_i(\lambda)$ – where $\lambda = \lambda(R_0, \mu, \alpha)$ guarantees that the effective distance accurately estimates the infection hitting times (see Supplementary Note S2 for the details) – outperforms all the other metrics for almost all the values of R_0 by a great margin. The correlation between the scores by the centrality metrics and the prevalence $\omega(t_{max})$ as a function of the basic reproductive number R_0 (with fixed $\mu = 0.2 \text{ d}^{-1}$, in unit of days) is shown in Fig. 5a. ViralRank is by far the best-performing metric for all the analyzed R_0 values. The scatter-plots between the scores by the analyzed centrality metrics and epidemic prevalence are reported, for $R_0 = 2$, in Fig. S10. The second-best performing metric is RWA, followed by k_c . The observed performance advantage of ViralRank can be ascribed to the fact that differently from the other metrics, ViralRank built directly on the random-walk effective distance which is an accurate estimate of the hitting time of a diffusive process on the network [38]. By extending the analysis to the whole accessible parameter space ($\beta > \mu$), the correlation between ViralRank and the epidemic prevalence stays larger than 0.8 for a large portion of the accessible space (Fig. 5b), and ViralRank is by far the best-performing metric in the whole accessible space (Fig. 5c), apart from a confined region close to the diagonal $\beta = \mu$. Importantly, as all real diseases reported in Table 10.2 by [28] have $R_0 \geq 2$, they all fall into the parameter region where ViralRank significantly outperforms all the other metrics – the region above the dashed line $R_0 = 2$ in Figs. 5(b,c).

DISCUSSION

In this work, we have introduced a new network centrality, called ViralRank, which quantifies the spreading ability of single nodes significantly better than existing metrics for both contact-networks and reaction-diffusion supercritical spreading. Our work is the first one that builds a centrality metric on analytic estimates of random-walk hitting times [38] and, at the same time, extensively validates the resulting centrality metric as a method to identify influential spreaders. We make the code to compute ViralRank available at https://github.com/kunda00/viralrank_centrality. Besides, we have connected ViralRank to the well-known Friedkin-Johnsen opinion formation model [2], and pointed out its difference with respect to the popular PageRank algorithm.

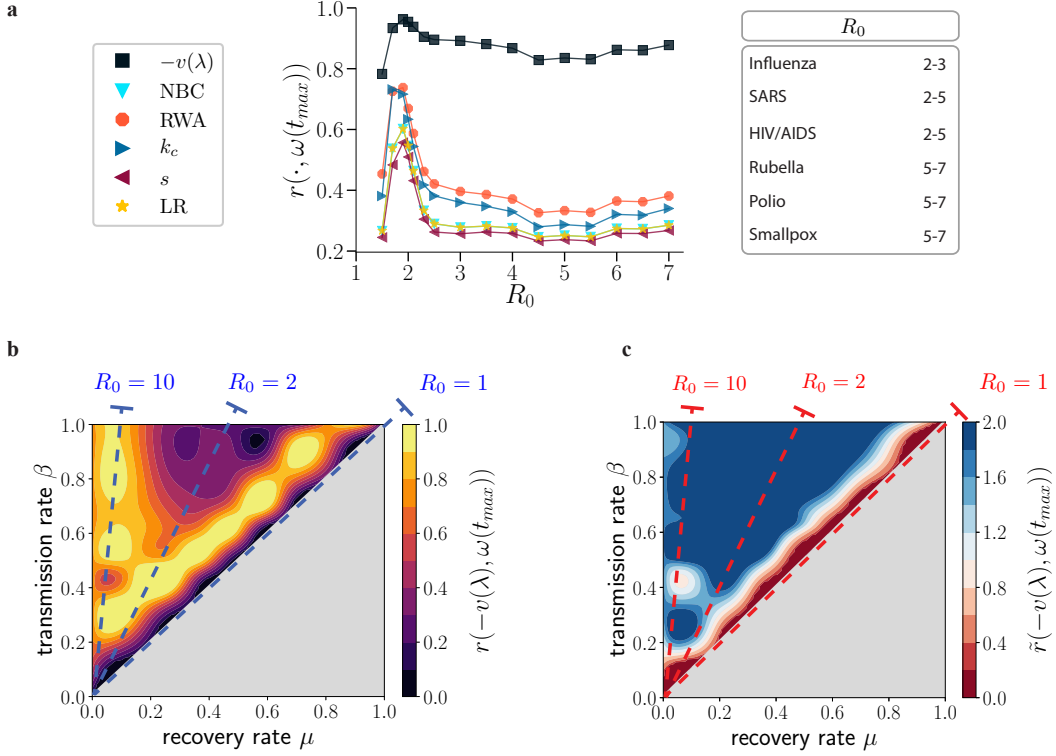


FIG. 5. Metapopulation spreading model: A comparison between nodes' centrality and prevalence $\omega(t_{max})$ for the U.S. domestic flight connections network. (a) Pearson's linear correlation between nodes' centrality and $\omega(t_{max})$ as a function of the basic reproductive number, at fixed recovery rate $\mu = 0.2 \text{ d}^{-1}$, in unit of days. The inset shows the known R_0 values for some real diseases (from Table 10.2 in [28]). (b) Pearson's linear correlation $r(-v(\lambda), \omega(t_{max}))$ between ViralRank score and epidemic prevalence for the non-trivial section of the accessible parameter space $\{\beta > \mu\}$. (c) Ratio \tilde{r} between the correlations of ViralRank and the score obtained by the best performing metric (RWA), ViralRank excluded. The dashed lines in panels (b-c) mark the lines of constant reproductive number.

Differently from most existing studies, our analysis involved the study of the whole parameter space of the target spreading dynamics. Our work emphasizes that differently from the common belief, the problem of identifying the influential spreaders in the supercritical regime is important for two main reasons. First, differently from what was previously thought [24, 27], there are large differences among the metrics' performance in this regime that are revealed by our analysis. Second, and most importantly, if we assume an SIR spreading dynamics, the propagation of real diseases and computer viruses falls in the supercritical parameter region. This points out that while studying the spreading at the critical point remains an important theoretical challenge [27], supercritical spreading processes are in fact likely to be of practical relevance for applications to real spreading processes.

We conclude by outlining future research directions opened by our methodology and results. It remains open to extend the effective distance [38] and ViralRank to temporal networks. This might be of extreme practical relevance inasmuch as real networks exhibit strong non-markovian effects which in turn heavily impact the properties of network diffusion processes [57–59]. Besides, the

SIR model provides a realistic yet simplified model of real diseases' spreading. Extending our results to more realistic spreading models is an important direction for future research; to this end, it will be critical to calibrate the spreading simulations with the parameters observed in real epidemics. While our work focused on a widely-used epidemic spreading model (SIR), an extensive validation of the metrics for social contagion processes [3, 23] remains elusive, yet important direction for future research.

Our paper focused on the identification of *individual* influential spreaders, in the sense that the simulated outbreaks always started from a single seed node. Identifying a set of multiple influential spreaders might require different methods with respect to those used to identify individual influential spreaders [15, 60]. Extending our results to spreading processes simultaneously initiated by more than one node is a non-trivial problem for future studies, yet relevant for real-world applications (such as targeted advertising and disease immunization) where it is typically more convenient to target a large number of potential influencers [8].

Finally, ViralRank leads us closer to the optimal solution of the influential spreaders identification in the

supercritical regime. While our results suggest that this regime is relevant for real spreading processes, it remains open to design, if at all possible, a universally best-performing metric that provides an optimal identification performance both in the supercritical and in the critical regime. For the SIR model, our findings confirm that the non-backtracking centrality [27] and LocalRank [15] are highly competitive around the critical point, yet their performance declines quickly in the supercritical regime. By contrast, the k -core centrality provides a better performance – yet sub-optimal with respect to ViralRank – in the supercritical regime. Understanding whether the effective distance can be used to build a centrality metric that is also competitive around the critical point is an intriguing challenge for future studies.

Appendix A: Details on the empirical datasets

The empirical datasets analyzed with the *contact-network* dynamics are: (1) [*Terrorists*] The terrorist network [61] which includes the terrorists (nodes) who belonged to the terroristic cell components centered around the 19 dead hijackers involved in the attacks at the World Trade Center of September 11th, 2001. Each link identifies a social or economic interaction between pairs of terrorists. (2) [*Email*] The emails contact network [62] where the nodes represent employees of a mid-sized manufacturing company. Two employees are connected by a network link if they exchanged at least one email in the year 2010. (3) [*Jazz*] The jazz musicians collaboration network [63] where the nodes represent jazz musicians, and the links represent their recorded collaborations between 1912 and 1940.; (4) [*NetScientists*] The largest component of the network scientists' co-authorship network [64] where the nodes are scientists working on network theory and experiments, and two scientists are linked if they co-authored at least one paper up to 2006. (5) [*Protein*] The network of interactions between the proteins contained in yeast [65]; each node represents a protein, and an edge represents a metabolic interaction between two proteins. (6) [*Facebook*] A Facebook friendship network [66] where the nodes represent Facebook users, and the links represent their friendship relations collected from survey participants using the Facebook mobile phone app.

For the simulations with the *metapopulation* model, we analyzed the weighted undirected network of the 500 most active commercial airports in the United States [67]. A pair of airports is connected if at least one flight was scheduled between them in 2002; each link is weighted by the total number of passengers who flew between those two airports in 2002.

Appendix B: ViralRank: interpretation and small λ expansion

The random-walk effective distance [38] can be written as

$$D_{ij}^{\text{RW}}(\lambda) = -\ln Z_{ij}(\lambda), \quad (\text{B1})$$

where

$$Z_{ij}(\lambda) = \sum_{n=1}^{\infty} e^{\ln H_{ij}(n)} e^{-\lambda n} = \langle e^{-\lambda n_{ij}} \rangle, \quad (\text{B2})$$

for $i \neq j$ and $Z_{ii}(\lambda) = 1$. In the last equation, $H_{ij}(n)$ is the hitting time probability of the random walk with transition probability matrix $P_{ij} = A_{ij} / \sum_k A_{ik}$, and n_{ij} is the random-walk hitting time [68]. The probability $H_{ij}(n)$ is defined recursively as [68] $H_{ij}(n) = \sum_{k \neq j} P_{ik} H_{kj}(n)$. The average $\langle \dots \rangle$ is taken over all the random-walk realizations of length $\{n\}$ weighted by the probability $H_{ij}(n)$ that selects only those walks that terminate once j is reached.

An interesting analogy with thermodynamics emerges. The constant λ can indeed be interpreted as an inverse temperature. Correspondingly, $Z_{ij}(\lambda)$ can be interpreted as a *partition function*, and the effective distance corresponds to a reduced free energy per temperature [38]. In this picture, each walk length n in the partition function can be interpreted as a single internal energy level n of the system; the quantity $H_{ij}(n) = e^{\ln H_{ij}(n)}$ quantifies the *relative weight* of the configurations of energy n – i.e. the walks of length n that terminate in j . Additionally, since H_{ij} is a probability, the (microcanonical) entropy $\mathcal{S}_{ij}^{\text{mic}}(n) = \ln H_{ij}(n)$ of the energy level n can be interpreted as the self-information (or surprisal) associated to the outcome of a random walker hitting node j for the first time after n steps starting from i . The total internal energy is then given by the average of the hitting time dampened by a decreasing exponential $\mathcal{U}_{ij} = \langle n_{ij} e^{-\lambda n_{ij}} \rangle / \langle e^{-\lambda n_{ij}} \rangle$, with the partition function at the denominator. The canonical entropy is obtained as $\mathcal{S}_{ij} = \lambda \mathcal{U}_{ij} - \lambda \mathcal{F}_{ij} = D_{ij}^{\text{RW}}(\lambda) = -\ln \langle e^{-\lambda n_{ij}} \rangle$ is the reduced free energy per temperature. Thus we find

$$\mathcal{S}_{ij} = \lambda \frac{\langle n_{ij} e^{-\lambda n_{ij}} \rangle}{\langle e^{-\lambda n_{ij}} \rangle} + \ln \langle e^{-\lambda n_{ij}} \rangle. \quad (\text{B3})$$

Using the expression of the effective distance in terms of the cumulants $\langle n_{ij} \rangle_c^k$ of the hitting time [38]

$$D_{ij}^{\text{RW}}(\lambda) = \sum_{k=1}^{\infty} (-1)^{k+1} \frac{\lambda^k \langle n_{ij} \rangle_c^k}{k!}, \quad (\text{B4})$$

the small- λ expansion of node i 's ViralRank score reads (up to a normalization constant)

$$v_i \underset{\lambda \rightarrow 0}{\approx} \lambda \sum_j (\langle n_{ij} \rangle + \langle n_{ji} \rangle) + \mathcal{O}(\lambda^2). \quad (\text{B5})$$

Here $\langle n_{ij} \rangle$ is the mean-first passage time (MFPT) from i to j defined recursively as $\langle n_{ij} \rangle = 1 + \sum_{k \neq j} P_{ik} \langle n_{kj} \rangle$ if $i \neq j$, zero otherwise [69].

In light of the analogy with thermodynamics outlined in the previous paragraph, as λ can be interpreted as an inverse temperature, the latter expression can be interpreted as a high-temperature expansion [70]. In this limit, the internal energy reduces to the MFPT, whereas the higher-order terms in the expansion (B4) give a vanishing contribution for small λ . The small- λ expansion shows that in the limit $\lambda \rightarrow 0$, apart from a uniform factor λ , node i 's ViralRank score tends to the average MFPT over the rest of the network

$$\tilde{v}_i \approx \sum_j (\langle n_{ij} \rangle + \langle n_{ji} \rangle). \quad (\text{B6})$$

Appendix C: The relation between the Friedkin-Johnsen (FJ) opinion formation model and ViralRank

In the Friedkin-Johnsen (FJ) linear model of opinion formation in networks, each node i starts with an opinion f_i ($\sum_i f_i = 1$), and recursively updates it according to the linear iterative equation

$$\mathbf{y}(t+1) = c \mathbf{U} \mathbf{y}(t) + (1-c) \mathbf{f} \quad (\text{C1})$$

where c is a model parameter, and \mathbf{U} denotes a row-stochastic interpersonal influence matrix. The final opinion y_i of a node i is linearly determined by the initial opinions f_j of all the other nodes $\{j\}$ through the linear relation $\mathbf{y}(c|\mathbf{f}) = \mathbf{V} \mathbf{f}$, where $\mathbf{V}(c) = (1-c)(\mathbf{I} - c\mathbf{U})^{-1}$. The matrix \mathbf{V} can be therefore interpreted as the total interpersonal effects matrix [71]. In the following, we set $\mathbf{U} = \mathbf{P}$, i.e. we assume that the interpersonal influence is completely determined by the network transition matrix \mathbf{P} .

Families of centrality metrics can be constructed from the matrix \mathbf{V} . An important one, referred to as total effects centrality by Friedkin [71], defines node i 's score as $\pi_j = \frac{1}{N} \sum_i V_{ij}$. As V_{ij} represents the total interpersonal influence of j on i , π_j represents the average effect of node j on the other nodes. Interestingly, as pointed out by Friedkin and Johnsen [72], in the case of interest here ($\mathbf{U} = \mathbf{P}$), this metric is exactly equivalent to Google's PageRank [40].

In terms of the FJ social influence model, the ViralRank centrality can be compactly written as

$$v_i(\lambda) = -\frac{1}{N} \sum_j \ln \left(y_i^{(j)}(e^{-\lambda}|\mathbf{f}^{(j)}) y_j^{(i)}(e^{-\lambda}|\mathbf{f}^{(i)}) \right), \quad (\text{C2})$$

where $\mathbf{f}^{(j)} = \mathbf{p}^{(j)} e^{-\lambda} / (1 - e^{-\lambda})$ is the initial opinion of the FJ model and the superscript (j) means that node j is removed from the vector; $y_i^{(j)}$ is the final opinion of i neglecting the contribution of node j , and analogously

for $y_j^{(i)}$. This equation is derived in the Supplementary Note S3. The FJ opinion-formation process that leads to $y_i^{(j)}$ – see Supplementary Note S3 – can be interpreted as follows: each node i starts with an "opinion" proportional to $p_i^{(j)} = P_{ij}$ (with $i \neq j$) which represents the random-walk probability of jumping from i to j in one time update. Each node iteratively updates its score by summing the probabilities P_{im} of its neighbors, j excluded, based on the FJ dynamics; the stationary state of this iterative process is $y_i^{(j)}$ which can be therefore interpreted as a (network-determined) effective transition probability P_{ij} . The ViralRank score v_i of a given node i therefore depends on all its effective transition probabilities $y_i^{(j)}$ and $y_j^{(i)}$.

Appendix D: The relation between Google's PageRank and network effective distance

Interestingly, a PageRank vector [48] of scores with non-uniform teleportation [73] can be also obtained by averaging a partition function. To show this, let us consider the partition function

$$\tilde{Z}_{ij}(\mathbf{P}, \lambda) = \sum_{k \neq j} (\mathbf{I} - e^{-\lambda} \mathbf{P})_{ik}^{-1} e^{-\lambda} P_{kj}. \quad (\text{D1})$$

Note that $\tilde{Z}_{ij}(\mathbf{P}^T) = \tilde{Z}_{ji}(\mathbf{P})$ (see Supplementary Note S4). This quantity differs from the partition function $Z_{ij}(\mathbf{P})$ defined as $Z_{ij}(\mathbf{P}) = \exp(-D_{ij}^{RW})$ (see Eq. (2)) as $\tilde{Z}_{ij}(\mathbf{P})$ considers all the walks that start in i and arrive in j . By contrast, being the moment generating function of the hitting time, the partition function $Z_{ij}(\mathbf{P})$ only consider the walks that end as soon as they arrive at the target j the first time.

By averaging the partition function \tilde{Z}_{ij} over the source nodes $\{i\}$, we obtain the vector $\tilde{\pi}_j = \frac{1}{N} \sum_i \tilde{Z}_{ij}$ which satisfies the PageRank equation

$$(\mathbf{I} - e^{-\lambda} \mathbf{P}^T) \tilde{\pi} = (1 - e^{-\lambda}) \tilde{\mathbf{g}}, \quad (\text{D2})$$

where

$$\tilde{g}_k = \frac{1}{N} \frac{e^{-\lambda}}{(1 - e^{-\lambda})} \sum_i P_{ik}. \quad (\text{D3})$$

Eq. (D2) therefore shows that PageRank with damping parameter $c = e^{-\lambda}$ and non-uniform teleportation vector [73] $\tilde{\mathbf{g}}$ can be recovered from the partition function \tilde{Z}_{ij} that also includes walks that hit the target nodes $\{j\}$ multiple times. By contrast, ViralRank is based on the effective distance that is the logarithm of a partition function that only includes the walks that terminate once they hit the arrival node. We argue that these differences lead to the better ViralRank's performance for the toy network of Fig. 2, and for the empirical networks (see Fig. S3) where PageRank is even outperformed by degree.

ACKNOWLEDGEMENTS

The authors thank Linyuan Lü for her detailed feedback on the manuscript and for several discussions on the topic and Giulio Iannelli for technical assistance in

producing Figure 1.

This work has partially been funded by the DFG / FAPESP, within the scope of the IRTG 1740 / TRP 2015/50122-0. M.S.M. acknowledges financial support from the Universität Zürich through the URPP Social Networks, and from the Swiss National Science Foundation Grant No. 200020-156188.

-
- [1] M. H. DeGroot, Journal of the American Statistical Association **69**, 118 (1974).
 - [2] N. E. Friedkin and E. C. Johnsen, The Journal of Mathematical Sociology **15**, 193 (1990).
 - [3] D. P. Maki and M. Thompson, *Mathematical models and applications: with emphasis on the social life, and management sciences*, Tech. Rep. (1973).
 - [4] R. Pastor-Satorras and A. Vespignani, *Evolution and structure of the Internet: A statistical physics approach* (Cambridge University Press, 2007).
 - [5] R. Pastor-Satorras, C. Castellano, P. Van Mieghem, and A. Vespignani, Reviews of modern physics **87**, 925 (2015).
 - [6] H. W. Hethcote, SIAM review **42**, 599 (2000).
 - [7] M. Granovetter, American Journal of Sociology **83**, 1420 (1978).
 - [8] E. Bakshy, J. M. Hofman, W. A. Mason, and D. J. Watts, in *Proceedings of the Fourth ACM International Conference on Web Search and Data Mining* (ACM, 2011) pp. 65–74.
 - [9] S. Pei, L. Muchnik, J. S. Andrade Jr, Z. Zheng, and H. A. Makse, Scientific reports **4**, 5547 (2014).
 - [10] Z.-K. Zhang, C. Liu, X.-X. Zhan, X. Lu, C.-X. Zhang, and Y.-C. Zhang, Physics Reports **651**, 1 (2016).
 - [11] N. E. Friedkin and F. Bullo, Proceedings of the National Academy of Sciences **114**, 11380 (2017).
 - [12] K. T. Eames and M. J. Keeling, Proceedings of the National Academy of Sciences **99**, 13330 (2002).
 - [13] D. Kempe, J. Kleinberg, and É. Tardos, in *Proceedings of the ninth ACM SIGKDD international conference on Knowledge discovery and data mining* (ACM, 2003) pp. 137–146.
 - [14] C. Kiss and M. Bichler, Decision Support Systems **46**, 233 (2008).
 - [15] L. Lü, D. Chen, X.-L. Ren, Q.-M. Zhang, Y.-C. Zhang, and T. Zhou, Physics Reports **650**, 1 (2016).
 - [16] A. Galeotti and S. Goyal, The RAND Journal of Economics **40**, 509 (2009).
 - [17] O. Hinz, B. Skiera, C. Barrot, and J. U. Becker, Journal of Marketing **75**, 55 (2011).
 - [18] D. J. Watts and P. S. Dodds, Journal of consumer research **34**, 441 (2007).
 - [19] R. Iyengar, C. Van den Bulte, and T. W. Valente, Marketing Science **30**, 195 (2011).
 - [20] P. Domingos and M. Richardson, in *Proceedings of the seventh ACM SIGKDD international conference on Knowledge discovery and data mining* (ACM, 2001) pp. 57–66.
 - [21] J. Leskovec, L. A. Adamic, and B. A. Huberman, ACM Transactions on the Web (TWEB) **1**, 5 (2007).
 - [22] R. Cohen, S. Havlin, and D. Ben-Avraham, Physical Review Letters **91**, 247901 (2003).
 - [23] J. Borge-Holthoefer and Y. Moreno, Physical Review E **85**, 026116 (2012).
 - [24] M. Kitsak, L. K. Gallos, S. Havlin, F. Liljeros, L. Muchnik, H. E. Stanley, and H. A. Makse, Nature physics **6**, 888 (2010).
 - [25] G. F. de Arruda, A. L. Barbieri, P. M. Rodríguez, F. A. Rodrigues, Y. Moreno, and L. da Fontoura Costa, Physical Review E **90**, 032812 (2014).
 - [26] F. Bauer and J. T. Lizier, EPL (Europhysics Letters) **99**, 68007 (2012).
 - [27] F. Radicchi and C. Castellano, Physical Review E **93**, 062314 (2016).
 - [28] A.-L. Barabási, *Network science* (Cambridge University Press, 2016).
 - [29] H. Liao, M. S. Mariani, M. Medo, Y.-C. Zhang, and M.-Y. Zhou, Physics Reports **689**, 1 (2017).
 - [30] L. Katz, Psychometrika **18**, 39 (1953).
 - [31] D. Chen, L. Lü, M.-S. Shang, Y.-C. Zhang, and T. Zhou, Physica a: Statistical mechanics and its applications **391**, 1777 (2012).
 - [32] A. Zeng and C.-J. Zhang, Physics Letters A **377**, 1031 (2013).
 - [33] J.-G. Liu, Z.-M. Ren, and Q. Guo, Physica A: Statistical Mechanics and its Applications **392**, 4154 (2013).
 - [34] L. Lü, T. Zhou, Q.-M. Zhang, and H. E. Stanley, Nature communications **7**, 10168 (2016).
 - [35] R. Pastor-Satorras and C. Castellano, Physical Review E **95**, 022301 (2017).
 - [36] G. Lawyer, Scientific reports **5**, 8665 (2015).
 - [37] P. Bonacich, Journal of Mathematical Sociology **2**, 113 (1972).
 - [38] F. Iannelli, A. Koher, D. Brockmann, P. Hövel, and I. M. Sokolov, Phys. Rev. E **95**, 012313 (2017).
 - [39] N. E. Friedkin, P. Jia, and F. Bullo, Sociological Science **3**, 444 (2016).
 - [40] S. Brin and L. Page, Computer networks and ISDN systems **30**, 107 (1998).
 - [41] D. J. Watts and S. H. Strogatz, nature **393**, 440 (1998).
 - [42] R. Pastor-Satorras and A. Vespignani, Physical review letters **86**, 3200 (2001).
 - [43] D. J. Watts, Proceedings of the National Academy of Sciences **99**, 5766 (2002).
 - [44] D. Brockmann and D. Helbing, Science **342**, 1337 (2013).
 - [45] We assume that the network is connected.
 - [46] To compare ViralRank’s performance with that of metrics that rank the nodes in order of *decreasing* score (e.g., degree), we use $-v$ in Figs. 3, 4 and 5. In this way, the nodes are again ranked in order of decreasing (yet increasing in modulus) score. To keep the terminology simple, we always refer to the correlation between $-v$ and node’s spreading ability as ViralRank’s performance.
 - [47] This MFPT is also known as global MFPT [74].
 - [48] D. Gleich, SIAM Review **57**, 321 (2015).

- [49] T. Martin, X. Zhang, and M. Newman, *Physical review E* **90**, 052808 (2014).
- [50] The epidemic threshold for the SIR model can be estimated within the degree-block approximation, i.e. assuming no degree correlations, as [75] $\beta_c = \langle k \rangle / (\langle k^2 \rangle - \langle k \rangle)$, where $k_i = \sum_j A_{ij}$ denotes the degree.
- [51] D. Balcan, B. Gonçalves, H. Hu, J. J. Ramasco, V. Colizza, and A. Vespignani, *Journal of computational science* **1**, 132 (2010).
- [52] P. Bajardi, C. Poletto, J. J. Ramasco, M. Tizzoni, V. Colizza, and A. Vespignani, *PloS one* **6**, e16591 (2011).
- [53] W. Van den Broeck, C. Gioannini, B. Gonçalves, M. Quagiotto, V. Colizza, and A. Vespignani, *BMC infectious diseases* **11**, 37 (2011).
- [54] M. Tizzoni, P. Bajardi, C. Poletto, J. J. Ramasco, D. Balcan, B. Gonçalves, N. Perra, V. Colizza, and A. Vespignani, *BMC medicine* **10**, 165 (2012).
- [55] V. Colizza, A. Barrat, M. Barthélemy, and A. Vespignani, *BMC Medicine* **5**, 1 (2007).
- [56] V. Colizza, A. Barrat, M. Barthélemy, and A. Vespignani, *Proceedings of the National Academy of Sciences of the United States of America* **103**, 2015 (2006).
- [57] M. Rosvall, A. V. Esquivel, A. Lancichinetti, J. D. West, and R. Lambiotte, *Nature Communications* **5** (2014).
- [58] I. Scholtes, N. Wider, R. Pfitzner, A. Garas, C. J. Tesse, and F. Schweitzer, *Nature Communications* **5**, 5024 EP (2014).
- [59] P. Holme, *Physical Review E* **94**, 022305 (2016).
- [60] F. Morone and H. A. Makse, *Nature* **524**, 65 (2015).
- [61] V. E. Krebs, *Connections* **24**, 43 (2002).
- [62] R. Michalski, S. Palus, and P. Kazienko, "Matching organizational structure and social network extracted from email communication," in *Business Information Systems: 14th International Conference, BIS 2011, Poznań, Poland, June 15-17, 2011. Proceedings*, edited by W. Abramowicz (Springer Berlin Heidelberg, Berlin, Heidelberg, 2011) pp. 97–206.
- [63] P. M. Gleiser and L. Danon, *Advances in complex systems* **6**, 565 (2003).
- [64] M. E. Newman, *Physical review E* **74**, 036104 (2006).
- [65] S. Coulomb, M. Bauer, D. Bernard, and M.-C. Marsolier-Kergoat, *Proceedings of the Royal Society B: Biological Sciences* **272**, 1721 (2005).
- [66] J. Leskovec and J. J. Mcauley, in *Advances in neural information processing systems* (2012) pp. 539–547.
- [67] V. Colizza, R. Pastor-Satorras, and A. Vespignani, *Nature Physics* **3**, 276 (2007).
- [68] J. R. Norris, *Markov Chains* (Cambridge University Press, 1998).
- [69] J. G. Kemeny and J. L. Snell, (1960).
- [70] G. Parisi, *Statistical Field Theory* (Addison-Wesley Pub. Co., 1988).
- [71] N. E. Friedkin, *American Journal of Sociology* **96**, 1478 (1991).
- [72] N. E. Friedkin and E. C. Johnsen, *Social Networks* **39**, 12 (2014).
- [73] R. Lambiotte and M. Rosvall, *Physical Review E* **85**, 056107 (2012).
- [74] V. Tejedor, O. Bénichou, and R. Voituriez, *Physical Review E* **80**, 065104 (2009).
- [75] A. Barrat, M. Barthélemy, and A. Vespignani, *Dynamical Processes on Complex Networks* (Cambridge University Press, 2008).
- [76] K.-i. Hashimoto, *Automorphic forms and geometry of arithmetic varieties.* , 211 (1989).
- [77] F. Krzakala, C. Moore, E. Mossel, J. Neeman, A. Sly, L. Zdeborová, and P. Zhang, *Proceedings of the National Academy of Sciences* **110**, 20935 (2013).
- [78] B. A. N. Travençolo and L. d. F. Costa, *Physics Letters A* **373**, 89 (2008).
- [79] J. L. Aron, M. O'leary, R. A. Gove, S. Azadegan, and M. C. Schneider, *Computers & Security* **21**, 142 (2002).
- [80] R. M. Anderson, R. M. May, and B. Anderson, *Infectious diseases of humans: dynamics and control*, Vol. 28 (Wiley Online Library, 1992).
- [81] L. Meyers, *Bulletin of the American Mathematical Society* **44**, 63 (2007).
- [82] J. O. Kephart, S. R. White, and D. M. Chess, *IEEE Spectrum* **30**, 20 (1993).
- [83] J. O. Kephart, G. B. Sorkin, D. M. Chess, and S. R. White, *Scientific American* **277**, 88 (1997).
- [84] The normalization of g_i also implies that π_i is normalized to unity.
- [85] This condition is always satisfied by definition of effective distance.
- [86] W. W. Zachary, *Journal of anthropological research* **33**, 452 (1977).
- [87] D. Lusseau, K. Schneider, O. J. Boisseau, P. Haase, E. Slooten, and S. M. Dawson, *Behavioral Ecology and Sociobiology* **54**, 396 (2003).
- [88] D. E. Knuth, *The Stanford GraphBase: a platform for combinatorial computing*, Vol. 37 (Addison-Wesley Reading, 1993).

Supplementary Material

Supplementary Note S1: Existing centrality metrics

Degree centrality, k , and strength centrality, s . The degree centrality k is arguably the simplest centrality measure, which is defined as the number of connections attached to each node. Given the adjacency matrix \mathbf{A} – $A_{ij} = 1$ if there is a connection between nodes i and j , zero otherwise – the degree centrality is the sum $k_i = \sum_j A_{ij}$. For weighted networks with weighted adjacency matrix \mathbf{W} – $W_{ij} \geq 0$ is the weight assigned to the connection between nodes i and j –, the previous definition is naturally extended by the strength centrality $s_i = \sum_j W_{ij}$.

k -core centrality, k_c . The k -core centrality[24] is obtained from the maximal connected subgraph composed of nodes that have at least k neighbors within the set itself. The k -core decomposition of the graph is an iterative procedure that classifies all nodes in shells of increasing connectivity. Each node is endowed with an integer k -core index k_c which equals the largest k value of k -cores to which the node belongs. This measure has been shown to outperform the degree centrality in the seminal work of Kitsak et al. [24] for the identification of influential spreaders.

LocalRank, LR . LocalRank is a centrality that considers both the nearest and the next nearest neighbors to fourth order [31]. It is defined for node i as

$$[LR]_i = \sum_k A_{ik} \sum_m A_{km} \sum_n A_{mn} (1 + \sum_r A_{nr}). \quad (\text{S1})$$

This metric has been shown to be competitive in the influential spreaders identification by the recent review article by Lü et al.[15].

Non-backtracking centrality, NBC . The non-backtracking centrality[49] is introduced to overcome the limitation of the eigenvector centrality by considering the Hashimoto or non-backtracking matrix [76, 77]. Given an abstract undirected network with E edges, we construct a directed version of it with $2E$ edges, where each original edge has been replaced by two directed ones pointing in opposite directions. The non-backtracking matrix B is the $2E \times 2E$ non-symmetric matrix, where each element corresponds to a pair of directed edges, defined as

$$B_{i \rightarrow j, k \rightarrow l} = \delta_{jk}(1 - \delta_{il}). \quad (\text{S2})$$

Thus the only non-zero elements of B are the ones defining non-backtracking paths of lengths two, from i to l with $j = k$ and $l \neq i$. From this the non-backtracking centrality is evaluated as

$$[NBC]_i = \sum_j A_{ij} v_{i \rightarrow j}, \quad (\text{S3})$$

where $v_{i \rightarrow j}$ is the eigenvector corresponding to the largest eigenvalue of the non-backtracking matrix B . For the Perron-Frobenius theorem the largest eigenvalue of B is always real and positive, and the the same holds for the components of the corresponding eigenvector. A much faster calculation of NBC can be carried out via the Ihara-Bass determinant as the first N elements of the leading left eigenvector of the $2N \times 2N$ matrix

$$\mathbf{B}' = \begin{pmatrix} \mathbf{0} & \mathbf{K} - \mathbf{I} \\ -\mathbf{I} & \mathbf{A} \end{pmatrix} \quad (\text{S4})$$

where $K_{ij} = \delta_{ij} k_i$ is the diagonal matrix with the degrees k_i as entries and $(\mathbf{I})_{ij} = \delta_{ij}$ is the identity matrix. Radicchi et al.[27] showed that the non-backtracking centrality is the most competitive metric to identify the influential spreaders for spreading processes around the critical point.

Random-walk accessibility, RWA . The (generalized) random-walk accessibility[25, 78] is a measure that quantifies the diversity of access of individual nodes via random walks. The accessibility is defined by the exponential of the Shannon entropy of the exponential transition probability matrix $\mathbf{M} = \exp(\mathbf{P})$ as

$$[RWA]_i = \exp \left(- \sum_j M_{ij} \ln M_{ij} \right) \quad (\text{S5})$$

By construction of the matrix \mathbf{M} , the accessibility penalizes longer walks. Its applicability is further limited by the critical assumption, which may not hold in real spreading scenarios, that the walkers select nodes with the same probability in each step. The metric has been shown to be competitive for the influential spreaders identification in geographically embedded networks [25].

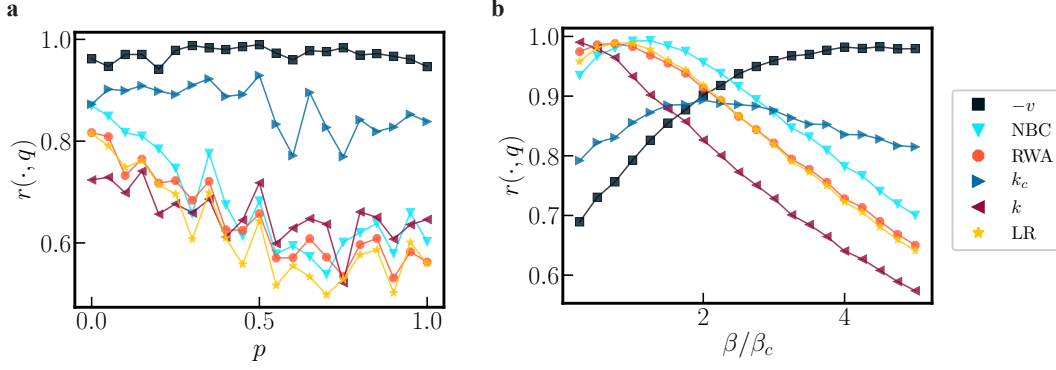


FIG. S1. Contact-network spreading model: A comparison between nodes' centrality and nodes' spreading ability q in synthetic networks composed of 100 nodes. (a) Pearson's linear correlation between node centrality and q as a function of the link rewiring probability p , at fixed $\beta/\beta_c = 4$. The extreme points $p = 0$ and $p = 1$ correspond to a scale-free and to a Poissonian topology, respectively. (b) Pearson's linear correlation between nodes' centrality and q as a function of β/β_c , at fixed $p = 0$ (scale-free topology).

Supplementary Note S2

Influential spreaders identification in synthetic contact networks

We analyze synthetic networks composed of $N = 100$ nodes and $L = 189$ links. To uncover how network topology affects the metrics' performance, we start from a network generated using the configuration model with connectivity distribution following a power-law $\mathcal{P}(k) \sim k^{-\gamma}$, with exponent $\gamma = 2$, and we replace a fraction p of its links with links that connects pairs of randomly selected nodes. In this way, we move continuously from a scale-free network ($p = 0$) to a random (Poissonian) topology ($p = 1$).

Fig. S1(a) shows the Pearson's correlation $r(\cdot, q)$ between nodes' spreading ability q and node score as a function of the shuffling probability p , for a fixed value of the ratio $\beta/\beta_c = 4$ and for all the considered centrality metrics. We find that all metrics but the k -core and ViralRank centrality decrease their correlation with the spreading ability as the network topology becomes more homogeneous (i.e., as p increases). This reflects the fact that for a random but homogeneous topology ($p = 1$), the spreading ability spans a narrower range of values and, as a consequence, it becomes increasingly harder for the metrics to accurately estimate q . ViralRank is the best performing metric for all the p values; nevertheless, we shall see in the following that the metrics' relative performance critically depends on β .

Fig. S1(b) shows the correlation $r(\cdot, q)$ as a function of β/β_c for the scale-free network ($p = 0$). First, we note that around the critical point $\beta = \beta_c$, LR, NBC and RWA all display a peak of maximum correlation with the spreading ability. This is in qualitative agreement with the fact that the NBC is expected to accurately estimate the size of the percolation giant component at the critical point[27], for locally tree-like graphs; at the same time, it remains interesting that LR and RWA display a similar behavior. This Figure also shows that above the critical point β_c , there exists an upper critical value $\beta_u > \beta_c$ such that ViralRank is always the best performing metric for $\beta \geq \beta_u$. Real data analysis shows that such point β_u exists for all the analyzed empirical datasets (see next paragraph).

We note that there is a sensible decrease in the overall performance of all metrics as β increases. This reflects the fact that as we approach the saturation value $\beta = 1$, the distribution of nodes' spreading ability q becomes narrower, making it harder for the metrics to quantify q . Nevertheless, we emphasize that for values of β as large as $\beta = 7\beta_c$ of this synthetic network, we are still able to observe significant differences among the metrics' performance. This indicates that the influential spreaders identification in the super-critical regime is still a non-trivial problem, an aspect that will also emerge in real data (see next paragraph).

To summarize, the results on synthetic networks show that in general the metrics' relative performance critically depends on the heterogeneity of the underlying network's topology and on the spreading dynamics parameters. The previous results also suggest that ViralRank significantly benefits from the spreading process being super-critical.

Are real spreading processes above or below the critical point? The optimal performance of ViralRank for $\beta > \beta_u$ motivates the following question: how far are real spreading processes from criticality? To address this question, we use publicly available ranges $[R_0^{min}, R_0^{max}]$ of observed reproductive numbers (Table 10.2 in [28]) for a set of real diseases, and publicly available values of observed transmission rates for a set of computer viruses – Table 2 in [79]. We find that, by assuming an SIR dynamics on the analyzed datasets, not only real cases fall into the super-critical regime, but a number of them are in the region $\beta > \beta_u$ where ViralRank outperforms the other metrics in identifying

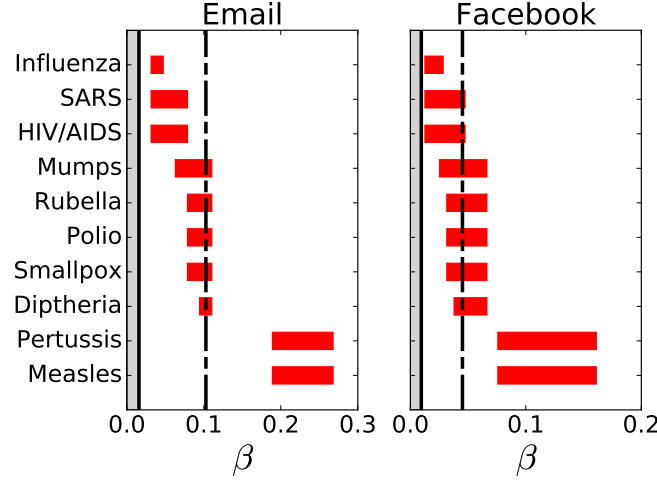


FIG. S2. Transmission-probability β values corresponding to real diseases in the email and the Facebook contact networks. The β ranges (red horizontal bars) match the ranges $[R_0^{min}, R_0^{max}]$ observed for real diseases, taken from Table 10.2 in [28]. By assuming $\mu = 1$, the R_0 values are converted into β values according to [81] $\beta = R_0 \langle k \rangle / (\langle k^2 \rangle - \langle k \rangle)$. The continuous and dashed vertical lines represent the epidemic threshold β_c and the point β_u such that ViralRank is the best-performing metric for $\beta > \beta_u$, respectively; gray and white colors fill the sub-critical and the super-critical interval, respectively.

influential spreaders. Below we provide the details of our analysis.

For a given disease, the reproductive number R_0 is defined as the number of secondary infections caused by a typical infected node in an entirely susceptible population [80]. For the SIR model in contact networks, one finds that in heterogeneous mean-field approximation [81] $R_0 \approx (\langle k^2 \rangle / \langle k \rangle - 1) \beta / \mu$. Therefore, we can use this formula and the observed ranges $[R_0^{min}, R_0^{max}]$ of reproductive numbers to estimate, for each real disease and each network of interest, the expected lower and upper bounds (denoted as β_{min} and β_{max} , respectively) for realistic values of β . We use this procedure to estimate the interval $[\beta_{min}, \beta_{max}]$ for the ten diseases of Table 10.2 in [28] in two contact-network datasets, emails and Facebook. The underlying assumption is that to some extent, these two networks can be considered as proxies for the social networks where the disease can spread.

We find that for both datasets, real diseases fall in the super-critical regime, and often in the region $\beta > \beta_u$ where ViralRank outperforms the other metrics in identifying the influential spreaders (see Fig. S2). For example, for the Facebook dataset, the lowest R_{min} value (Influenza, SARS, HIV/AIDS, $R_0^{min} = 2$) leads to $\beta_{min} = 2 \beta_c$, which lies still below $\beta_u = 4.75 \beta_c$. On the other hand, the upper value of β for SARS and HIV/AIDS lies above β_u ($\beta_{max} = 5 \beta_c$). The β ranges for the diseases with the largest R_0^{min} (Measles, Pertussis, $R_0^{min} = 12$) lie well above β_u ($\beta_{min} = 12 \beta_c$ and $\beta_{max} = 17 \beta_c$ for such diseases).

Values of the transmission probability for some computer viruses [4, 82, 83] can be found in Table 2 from [79]. All the non-zero values reported in that table lie well above the critical point β_c for the email dataset. The Word Macro virus ($\beta = 0.7$) falls in the region where ViralRank significantly outperforms the other metrics; the Excel Macro virus ($\beta = 0.1$) falls below but close to the point $\beta_u = 0.103$, whereas the Generic.exe virus falls in the region where the k -core centrality is the best performing metric.

These examples indicate that by assuming a SIR dynamics, we expect the propagation of real diseases and computer viruses to be a super-critical diffusion process. We acknowledge that our argument above is simplified, as it assumes a free propagation of the disease (i.e., no external intervention aimed at limiting the impact of the disease) on an isolated population, which is unlikely to happen in the propagation of real diseases. Nevertheless, our assumptions are the same as those of all previous studies [15, 24, 27, 34] that compared the performance of metrics for the influential spreaders identification based on the SIR diffusion model. Our argument therefore shows that, in the usual setting for benchmarking metrics for the influential spreaders identification, the propagation of real diseases and computer viruses falls in the super-critical regime, and ViralRank is often the best performing metric in identifying the influential spreaders. A study of the problem in a more realistic setting goes beyond the scope of this work as it would require a more complex model of propagation, an accurate calibration of model parameters, and the possibility of external intervention (such as vaccination and travel restriction in the case of diseases).

Equations of the SIR dynamics. Mathematically, we describe epidemic processes in the metapopulation model for the time independent populations \mathcal{N}_j as follows. We denote by \mathcal{S}_j , \mathcal{I}_j and \mathcal{R}_j the number of individuals who belong to population j who are in the susceptible, infected, and removed state, respectively – as a consequence, $\mathcal{N}_j = \mathcal{S}_j^{(t)} + \mathcal{I}_j^{(t)} + \mathcal{R}_j^{(t)}$. The correspondent normalized quantities are denoted as $\rho_j^{\mathcal{X}} = \mathcal{X}_j / \mathcal{N}_j$, where the place-holder variable \mathcal{X} can represent each of the three possible compartments: $\mathcal{X} = \{\mathcal{S}, \mathcal{I}, \mathcal{R}\}$. As for the case of epidemics on contact networks the quantity $\rho_j^{\mathcal{I}}(t)$ defines the probability that node j is infected at time t . The time evolution of the occupation densities is governed by the dynamics which consists of the sum of a diffusion term $\Omega(\{\rho_j^{\mathcal{X}}\})$, known as the transport operator [75], and a reaction term $K^{\mathcal{X}}(\beta, \mu, \{\rho_j\})$ which include the transmission and recovery rates β and μ . Hence, $\partial \rho_j^{\mathcal{X}} / \partial t = \Omega(\{\rho_j^{\mathcal{X}}\}) + K^{\mathcal{X}}(\beta, \mu, \{\rho_j\})$. We are assuming that the nodes strengths $s_j = \sum_k W_{jk}$ and the populations are proportional via a diffusion rate $\alpha = s_j / \mathcal{N}_j$. Thus the transport operator can be written without the explicit dependence on the populations size as $\Omega(\{\rho_j^{\mathcal{X}}\}) = \alpha \sum_i P_{ji} (\rho_i^{\mathcal{X}} - \rho_j^{\mathcal{X}})$, where $P_{ij} = W_{ij} / s_i = P_{ji} s_j / s_i$ is the transition probability matrix. The strength vector is then the equilibrium distribution of the Markov chain with states defined by the nodes. With this assumption the populations size is not necessary for the simulation of the reaction-diffusion process. The full dynamics is then described by the set of non-linear differential equations

$$\begin{cases} \frac{\partial \rho_j^{\mathcal{S}}}{\partial t} = \Omega(\{\rho_j^{\mathcal{S}}\}) - \beta \rho_j^{\mathcal{S}} \rho_j^{\mathcal{I}} \\ \frac{\partial \rho_j^{\mathcal{I}}}{\partial t} = \Omega(\{\rho_j^{\mathcal{I}}\}) + \beta \rho_j^{\mathcal{S}} \rho_j^{\mathcal{I}} - \mu \rho_j^{\mathcal{I}} \end{cases} \quad (\text{S6})$$

Choice of the threshold time t_{max} . For this model, we use the outbreak size at a given threshold time t_{max} as a ground-truth estimate of node influence in the metapopulation dynamics. The threshold time t_{max} is set as half of the characteristic time for travel given by the inverse of the diffusion rate $\alpha = 0.003 \text{ d}^{-1}$ and, since higher transmission rates correspond to lower infection hitting times, normalized by the basic reproductive number of the infection; i.e. $t_{max}(R_0) = (2R_0\alpha)^{-1}$. That defines the prevalence $\omega(t_{max})$ used instead of the spreading ability for the metapopulation model. The results obtained with this choice of t_{max} are little sensitive to the exact choice of t_{max} as long as t_{max} is sufficiently large (see Fig. S11).

Dependence of ViralRank's parameter λ on the dynamics parameters. The definition of ViralRank for contact networks takes into account a formal limit of vanishing λ . In this limit, the ViralRank score of a node is equal to the average mean first-passage time of a random walk. By contrast, for a metapopulation dynamics, the parameter λ has a direct relation with the dynamics parameters R_0, μ, α : $\lambda(R_0, \mu, \alpha) = \ln[(R_0 - 1)\mu / \alpha e^{-\gamma_e}]$. Here $R_0 = \beta / \mu$ is the basic reproductive number of homogeneous mixing epidemics, μ and α the recovery and diffusion rates respectively and γ_e the Euler-Mascheroni constant. This relation guarantees that the effective distance D_{ij}^{RW} is highly correlated with the hitting time of the spreading process; as a consequence, for $\lambda = \lambda(R_0, \mu, \alpha)$, ViralRank is an accurate proxy for the average hitting time of the metapopulation spreading process. Inverting the previous relation yields $R_0 = 1 + \alpha / \mu e^{\lambda + \gamma_e}$. Thus, in order to have a positive λ , condition necessary for the random-walk effective distance to be defined in the first place, we additionally require that the basic reproductive number in our simulations always satisfies $R_0 \geq 1 + \alpha / \mu e^{\gamma_e}$. However, this additional constraint only excludes a limited interval of values from our analysis; for example, when $\mu = 0.2 \text{ d}^{-1}$ (value used in Fig.5a in the main text), the threshold is given by $R_0 \geq 1.027$.

Supplementary Note S3: The relation between ViralRank and the Friedkin-Johnsen (FJ) opinion formation model

In the Friedkin-Johnsen (FJ) linear model of opinion formation in social networks, each node i starts with an opinion f_i ($\sum_i f_i = 1$), and recursively updates it according to the linear iterative equation

$$\mathbf{y}(t+1) = c \mathbf{U} \mathbf{y}(t) + (1-c) \mathbf{f} \quad (\text{S7})$$

where c is a model parameter, and \mathbf{U} denotes a row-stochastic interpersonal influence matrix. In the following, as in the main text, we assume $\mathbf{U} = \mathbf{P}$:

$$\mathbf{y}(t+1) = c \mathbf{P} \mathbf{y}(t) + (1-c) \mathbf{f}. \quad (\text{S8})$$

Component by component, the previous equation reads

$$y_i(t+1) = c \sum_j P_{ij} y_j(t) + (1-c) f_i = \frac{c}{k_i} \sum_j A_{ij} y_j(t) + (1-c) f_i. \quad (\text{S9})$$

The previous equation has a simple interpretation: each node starts with an opinion f_i , and recursively updates it by averaging its neighbors' opinions.

To connect the FJ model with ViralRank, it is instrumental to consider a $(N-1) \times (N-1)$ reduced matrix $\mathbf{P}^{(j)}$ obtained from \mathbf{P} by removing the j -th row and column. The FJ opinion formation process associated with the reduced matrix $\mathbf{P}^{(j)}$ reads

$$\mathbf{y}^{(j)}(t+1) = c\mathbf{P}^{(j)}\mathbf{y}^{(j)}(t) + (1-c)\mathbf{f}^{(j)}, \quad (\text{S10})$$

and where $\mathbf{y}^{(j)}$ and $\mathbf{f}^{(j)}$ are $(N-1)$ -dimensional vectors. By writing the previous equation component by component, we obtain:

$$y_i^{(j)}(t+1) = c \sum_{m \neq j} P_{im} y_m^{(j)}(t) + (1-c) f_i^{(j)} = \frac{c}{k_i} \sum_{m \neq j} A_{im} y_m^{(j)}(t) + (1-c) f_i^{(j)}. \quad (\text{S11})$$

Eq. (S11) has a similar interpretation as equation (S9): each node starts with an opinion $f_i^{(j)}$, and recursively updates it by considering its neighbors' opinions. Differently from equation (S9), node j 's opinion does not contribute to the other nodes opinions. The stationary opinions $\mathbf{y}^{(j)}(c|\mathbf{f}^{(j)})$ of the nodes satisfy the equation

$$\mathbf{y}^{(j)}(c|\mathbf{f}^{(j)}) = c\mathbf{P}^{(j)}\mathbf{y}^{(j)}(c|\mathbf{f}^{(j)}) + (1-c)\mathbf{f}^{(j)}, \quad (\text{S12})$$

which is solved by

$$\mathbf{y}^{(j)}(c|\mathbf{f}^{(j)}) = (\mathbf{I}^{(j)} - c\mathbf{P}^{(j)})^{-1}(1-c)\mathbf{f}^{(j)}. \quad (\text{S13})$$

If $\mathbf{f}^{(j)} = \mathbf{f}^{(j)}(c) = c\mathbf{p}^{(j)}/(1-c)$, and $c = e^{-\lambda}$ (see main text for the definitions of $\mathbf{p}^{(j)}$ and λ), we obtain

$$\mathbf{y}^{(j)}(c|\mathbf{f}^{(j)}) = (\mathbf{I}^{(j)} - c\mathbf{P}^{(j)})^{-1} e^{-\lambda} \mathbf{p}^{(j)}; \quad (\text{S14})$$

as the right-hand side of the equation is exactly equal to the negative exponential of effective distance (compare with Eq. (2) of the main text), we obtain

$$y_i^{(j)}(e^{-\lambda}|\mathbf{f}^{(j)}(e^{-\lambda})) = e^{-D_{ij}^{\text{RW}}(\lambda)}. \quad (\text{S15})$$

From the definition of ViralRank (Eq. (1) in main text), Eq. (9) in main text follows.

Supplementary Note S4: Deriving PageRank from the network partition function

The PageRank vector is defined as the stationary density of a random-walk in discrete time on a graph, and is described by the master equation

$$\pi_i(t+1) = c \sum_j \pi_j(t) P_{ji} + (1-c) g_i, \quad (\text{S16})$$

where $c \in (0, 1)$ is the damping parameter, \mathbf{g} is the *preference* vector normalized to unity ($\sum_i g_i = 1$), and \mathbf{P} is the row-stochastic transition probability matrix[84]. The constant $(1-c)$ that multiplies the preference vector \mathbf{g} gives the probability to jump to any random state, while the entry g_i gives the conditional probability to teleport precisely to state i . The stationary solution π of Eq. (S16) reads[48]

$$\pi = (\mathbf{I} - c\mathbf{P}^T)^{-1} (1-c)\mathbf{g}. \quad (\text{S17})$$

In the most commonly used version of PageRank $g_i = 1/N$, $\forall i$, is the uniform distribution vector and $c = 0.85$. Variants of this choice that consider a node dependent preference vector have been considered in [73].

a. PageRank in the original graph from the effective distance partition function The PageRank score of a node is essentially a measure of how easy it is to reach a node with a random walk process. It is thus tempting to try to recover the PageRank vector of scores by modifying the effective distance in order to make it a measure of the reachability of a node for a diffusion process started from another node. The partition function of effective distance reads (see also equations (2) and (4) in main text)

$$Z_{ij}(\mathbf{P}, \lambda) = \sum_{k \neq j} \left(\mathbf{I}^{(j)} - e^{-\lambda} \mathbf{P}^{(j)} \right)_{ik}^{-1} e^{-\lambda} p_k^{(j)}. \quad (\text{S18})$$

In the previous equation $\mathbf{P}^{(j)}$ and $\mathbf{I}^{(j)}$ are the $(N-1) \times (N-1)$ submatrices of the Markov matrix $(\mathbf{P})_{ij} = A_{ij} / \sum_k A_{ik}$ and of the identity matrix $(\mathbf{I})_{ij} = \delta_{ij}$, respectively, obtained by excluding the j th row and j th column; $\mathbf{p}^{(j)}$ is the j th column of \mathbf{P} after removing the j th component.

Next we prove equation (11) of the main text, which defines PageRank with non-uniform teleportation vector in the original graph. This is done by defining the new partition function

$$\tilde{Z}_{ij}(\mathbf{P}, \lambda) = \sum_{k \neq j} (\mathbf{I} - e^{-\lambda} \mathbf{P})_{ik}^{-1} e^{-\lambda} P_{kj}. \quad (\text{S19})$$

Contrary to the partition function of equation (S18), where only walks that terminate in j are considered, in equation (S19) also those walks that cross multiple times the target j are considered.

First we note that by rearranging the sum

$$\begin{aligned} \tilde{Z}_{ij}(\mathbf{P}^T, \lambda) &= \sum_{k \neq j} \sum_{n=0}^{\infty} (e^{-\lambda} \mathbf{P}^T)_{ik}^n e^{-\lambda} P_{kj}^T \\ &= \sum_{m \neq j} \sum_{n=0}^{\infty} \sum_{k \neq j} e^{-\lambda} P_{jk} (e^{-\lambda} \mathbf{P})_{km}^{n-1} e^{-\lambda} P_{mi} \\ &= \sum_{m \neq j} \sum_{n=0}^{\infty} (e^{-\lambda} \mathbf{P})_{jm}^n e^{-\lambda} P_{mi} \\ &= \tilde{Z}_{ji}(\mathbf{P}, \lambda). \end{aligned} \quad (\text{S20})$$

By averaging the partition function, equation (S19), over the source nodes $\{i\}$ we obtain the vector

$$\tilde{\pi}_j = \frac{1}{N} \sum_i \tilde{Z}_{ji}(\mathbf{P}^T, \lambda) = \sum_{k \neq i} (\mathbf{I} - e^{-\lambda} \mathbf{P}^T)_{jk}^{-1} \frac{1}{N} \sum_i e^{-\lambda} P_{ki}^T. \quad (\text{S21})$$

If no self-loops are present we can include node i in the sum to get the PageRank equation (S17)

$$\tilde{\pi} = (\mathbf{I} - e^{-\lambda} \mathbf{P}^T)^{-1} (1 - e^{-\lambda}) \tilde{\mathbf{g}}, \quad (\text{S22})$$

where the dumping parameter is $c = e^{-\lambda}$ and the non-uniform preference vector is defined as

$$\tilde{g}_k = \frac{1}{N} \frac{e^{-\lambda}}{(1 - e^{-\lambda})} \sum_i P_{ik}. \quad (\text{S23})$$

Additionally we can impose the standard normalization by requiring that $\sum_k g_k = 1$ and rescale the whole PageRank equation (S22) by the normalization factor $(1 - e^{-\lambda})/e^{-\lambda}$, so that the new quantity $\tilde{\pi}'_k$ is correctly normalized to unity, as for equation (S17).

b. PageRank in the subgraph from the partition function of effective distance In this section we show that a PageRank in the $(N-1)$ sub-graph can be obtained directly from the effective distance partition function. To do this, we replace \mathbf{P} with \mathbf{P}^T in the definition of the partition function (S18), obtaining a modified partition function $Z_{ij}(\mathbf{P}^T, \lambda)$. As we will show next, the modified partition function defines for each target node j a PageRank score, with *smart* teleportation vector[73] given by $g_k^{(j)} = p_k^{T(j)} e^{-\lambda} / (1 - e^{-\lambda})$, evaluated in a network where the target node j has been removed, and where $p_k^{T(j)}$ is the j th row of \mathbf{P} with element j removed. In particular, let us consider the quantity $z_i^{(j)} = Z_{ij}(\mathbf{P}^T, \lambda) / \sum_{k \neq j} Z_{kj}(\mathbf{P}^T, \lambda)$, where $Z_{ij}(\mathbf{P}^T, \lambda) = \exp(-D_{ij}^{\text{RW}}(\mathbf{P}^T, \lambda))$. The equivalence theorem[48] states that for[85] $\lambda > 0$ the vector solution $\mathbf{z}^{(j)}$ of the matrix equation

$$z_i^{(j)} = \sum_{k \neq j} (\mathbf{I}^{(j)} - e^{-\lambda} \mathbf{Q}^{(j)})_{ik}^{-1} (1 - e^{-\lambda}) g_k^{(j)}. \quad (\text{S24})$$

is the solution of the PageRank problem defined in the $(N-1)$ -dimensional graph, provided that $g_k^{(j)} \geq 0, \forall k$. Here $\mathbf{Q}^{(j)} = \mathbf{P}^{T(j)} + \mathbf{g}^{(j)} (\mathbf{e}^{(j)T} - \mathbf{e}^{(j)T} \mathbf{P}^{T(j)})$ is the $(N-1) \times (N-1)$ column-stochastic matrix of a random walk in the $(N-1)$ -dimensional network constructed by removing node j . The *smart* teleportation vector $g_k^{(j)} = p_k^{T(j)} / \sum_{l \neq j} p_l^{T(j)} = p_k^{T(j)}$ is obtained by normalizing the j th row with element j removed of the original $N \times N$ row-stochastic matrix \mathbf{P} . Since $g_k^{(j)}$ has entries all positive or vanishing but never negative, by construction the hypothesis of the theorem are satisfied. We

conclude that the vector $z_i^{(j)}$, obtained by normalizing the negative exponential of effective distance with transposed transition matrix, is PageRank on the $(N - 1)$ subgraph obtained from the original one. This PageRank introduces a non-uniform probability for the navigation in the network, given by the vector $\mathbf{g}^{(j)}$ that maintains the information about the nodes importance. This particularity could be useful for modeling real-world navigation, where some web pages are more likely to be selected than other ones.

1. Supplementary Figures and Tables

	N	L	D	C	$\langle k \rangle$	$\langle k^2 \rangle$	β_c	β_u/β_c	Ref.
Karate	34	78	5	0.57	4.59	35.65	0.1477	2.50	[86]
Terrorists	62	152	5	0.49	4.90	40.03	0.1396	2.50	[61]
Dolphins	62	159	8	0.26	5.13	34.90	0.1723	2.00	[87]
LesMiserables	77	254	5	0.57	6.60	79.53	0.0905	3.50	[88]
Email	167	3250	5	0.59	38.92	2508.78	0.0158	6.50	[62]
Jazz	198	2742	6	0.62	27.70	1070.24	0.0266	4.25	[63]
Celegans	297	2148	5	0.29	14.04	365.70	0.0399	5.75	[41]
NetScientists	379	914	17	0.74	1.15	9.22	0.1424	2.00	[64]
Usa	500	2980	7	0.62	11.92	641.12	0.0189	8.00	[67]
Proteins	1458	1948	19	0.07	2.08	14.85	0.1632	2.25	[65]
Facebook	4039	88234	8	0.61	43.69	4656.14	0.0095	4.75	[66]
PowerGrid	4941	6594	46	0.08	2.67	10.33	0.3483	1.50	[41]

TABLE S1. Structural properties of all the datasets analyzed. The different columns are the number of nodes and links N and L , the diameter D , the clustering C , the first and second moment of the degree distribution $\langle k \rangle = 1/N \sum_i k_i$ and $\langle k^2 \rangle = 1/N \sum_i k_i^2$ and the epidemic threshold β_c at $\mu = 1$; the last two columns report the threshold value β_u above which ViralRank outperforms all the other metrics and the corresponding reference.

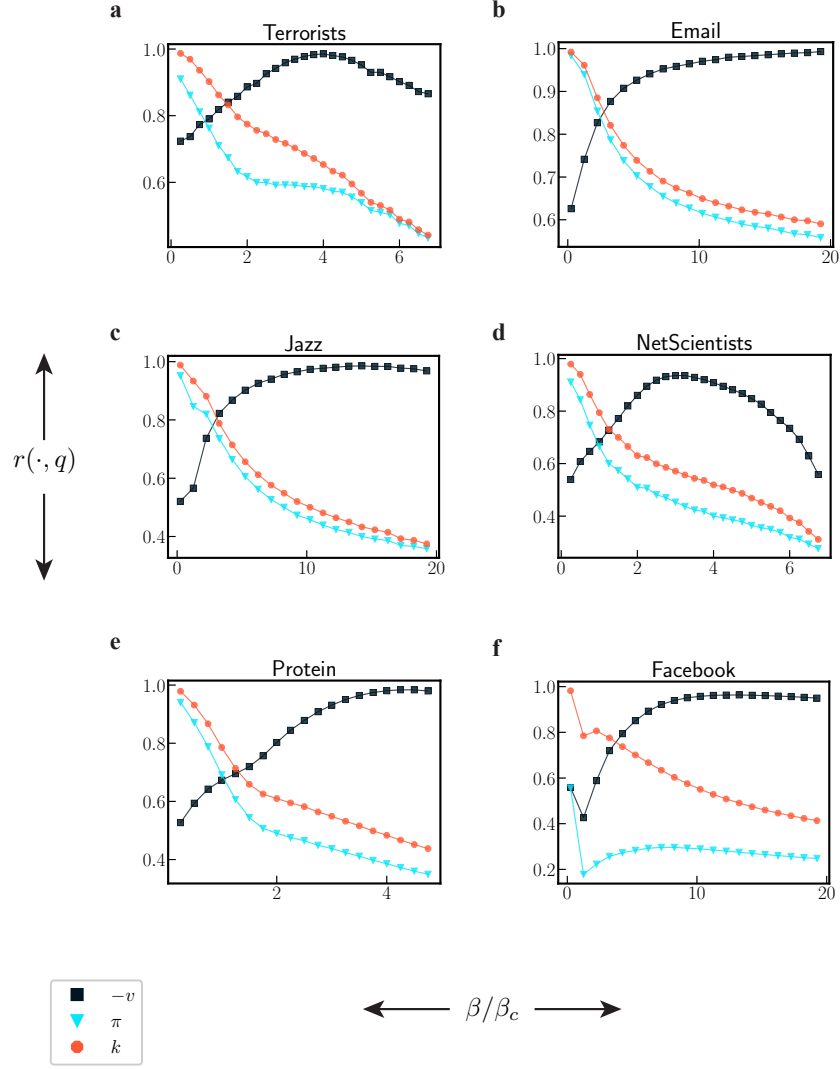


FIG. S3. Contact-network spreading model: a comparison between nodes' centrality and node spreading capacity q in the real networks analyzed in the main text. The figures represent the Pearson's linear correlation r between nodes' centrality and nodes' spreading capacity q . Differently from the main text (Fig. 3), the metrics considered here are ViralRank v ; PageRank [48] π with dumping parameter $c = 0.85$; degree centrality k . The panels represent the results for the following datasets: (a) 9/11 terrorists, (b) emails, (c) jazz collaborations, (d) network scientists co-authorships, (e) protein interactions and (f) Facebook friendships. The PageRank π performance is qualitatively similar to that of the degree centrality: the PageRank metrics outperform ViralRank in the small- β region, and they are outperformed as β becomes sufficiently large.

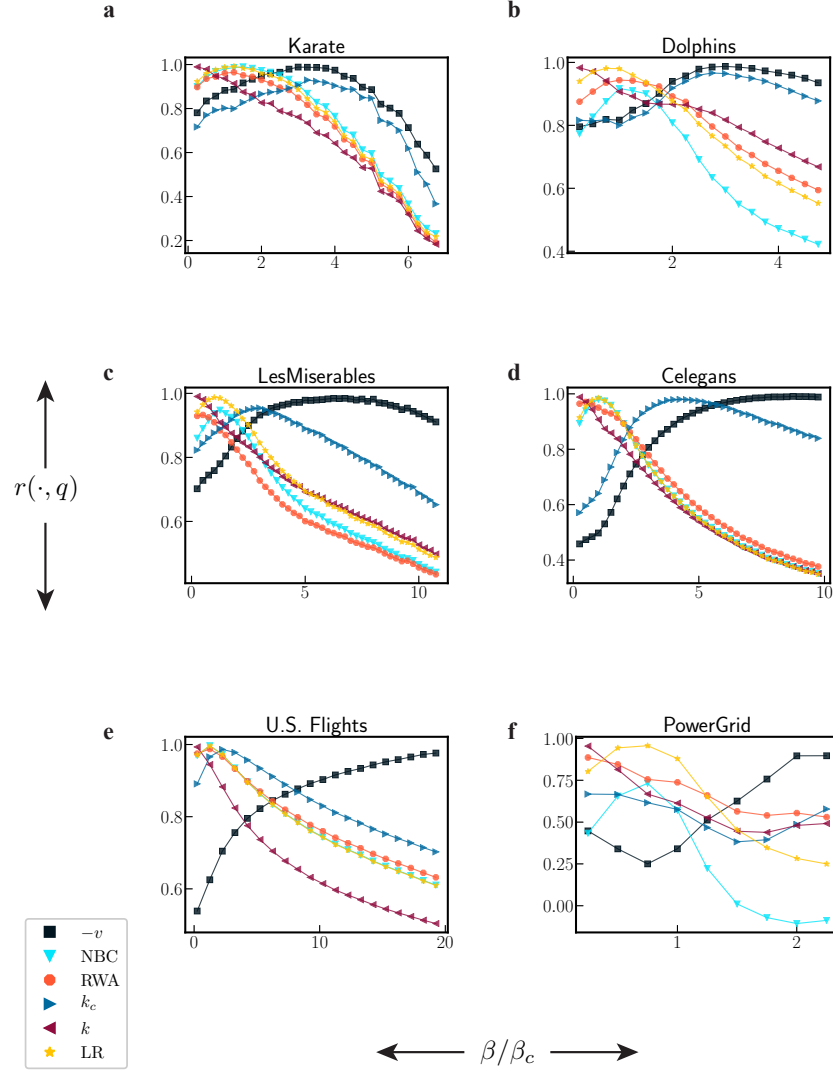


FIG. S4. Contact-network spreading model: a comparison between nodes' centrality and nodes' spreading ability q in real networks. Pearson's linear correlation between nodes' centrality and q as a function of β/β_c for (a) karate club friendships, (b) dolphins interactions, (c) les miserables characters co-appearances, (d) C.elegans neural connections, (e) U.S. flights and (f) U.S. powergrid supply lines.

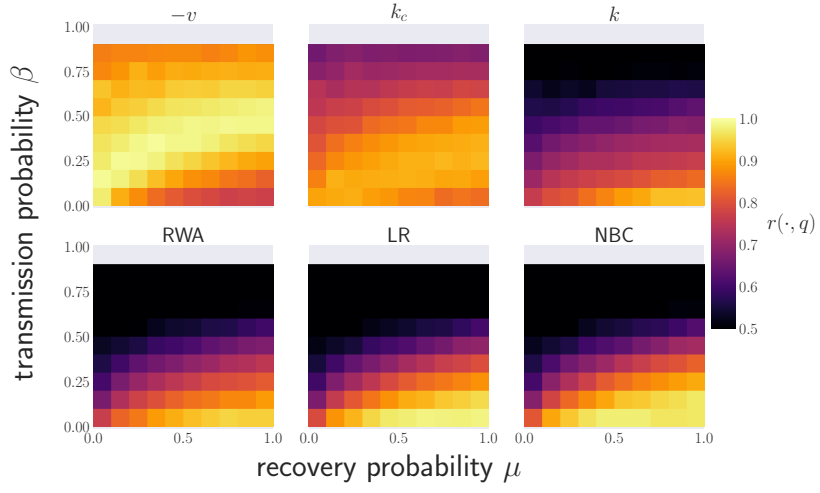


FIG. S5. Correlation heatmaps in the full parameter space (β, μ) for 9/11 terrorists network.

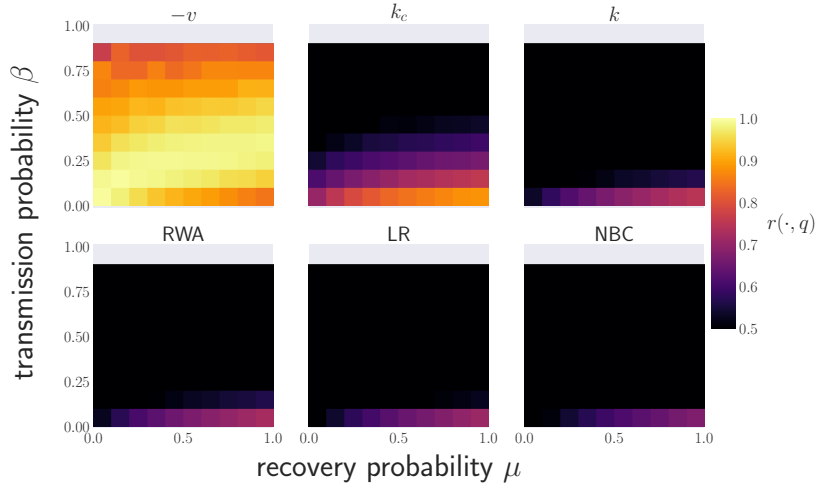


FIG. S6. Correlation heatmaps in the full parameter space (β, μ) for jazz collaborations network.

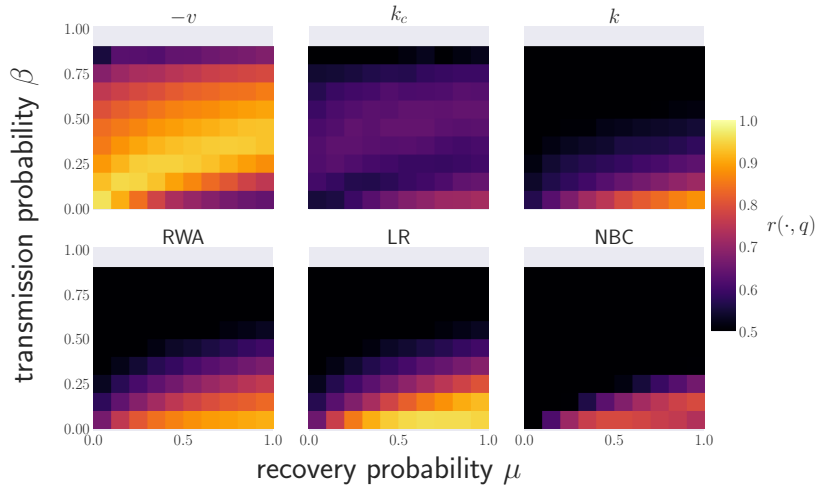


FIG. S7. Correlation heatmaps in the full parameter space (β, μ) for network scientists co-authorships network.

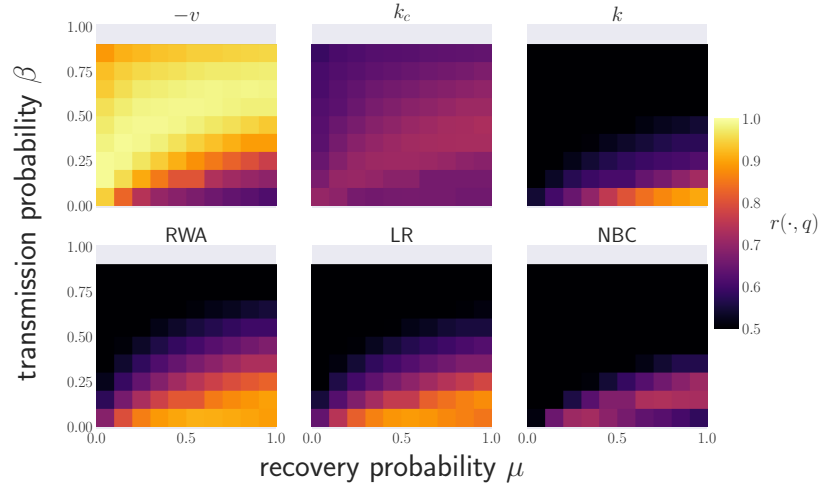


FIG. S8. Correlation heatmaps in the full parameter space (β, μ) for protein interaction network.

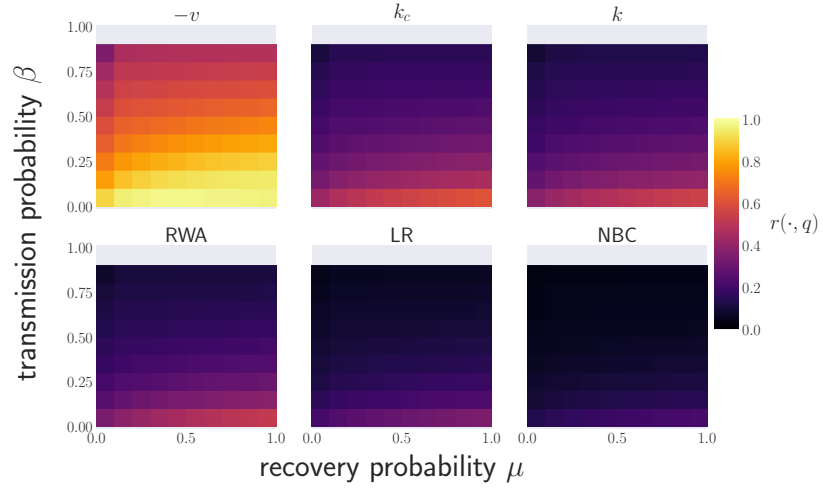


FIG. S9. Correlation heatmaps in the full parameter space (β, μ) for Facebook friendships network.

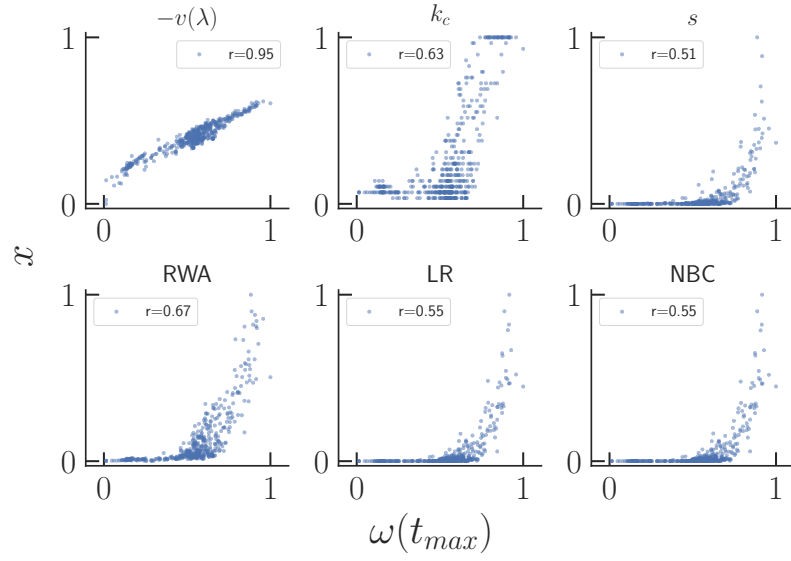


FIG. S10. Scatter plot of the nodes' centrality scores x as a function of the nodes' spreading ability quantified by the prevalence $\omega(t_{max})$ at time $t_{max} = (2\alpha R_0)^{-1}$ for $R_0 = 2.0$ and $\alpha = 0.003 \text{ d}^{-1}$. For each axis, the values are normalized by the maximum value.

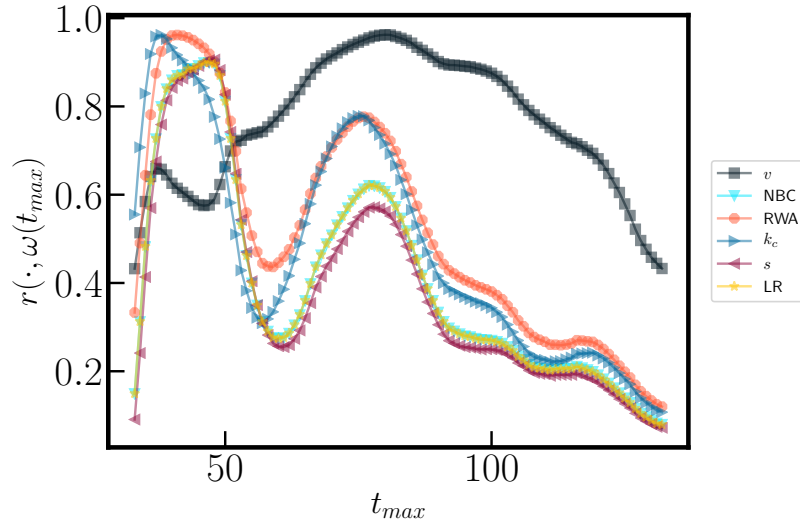


FIG. S11. Benchmark performance with Pearson correlation coefficient between prevalence $\omega(t_{max})$ and centrality measures as a function of the observation time t_{max} . Here the observation time t_{max} is varied by keeping the value of basic reproductive number $R_0 = 2.0$ fixed.

-
- [1] M. H. DeGroot, Journal of the American Statistical Association **69**, 118 (1974).
 - [2] N. E. Friedkin and E. C. Johnsen, The Journal of Mathematical Sociology **15**, 193 (1990).
 - [3] D. P. Maki and M. Thompson, *Mathematical models and applications: with emphasis on the social life, and management sciences*, Tech. Rep. (1973).
 - [4] R. Pastor-Satorras and A. Vespignani, *Evolution and structure of the Internet: A statistical physics approach* (Cambridge University Press, 2007).
 - [5] R. Pastor-Satorras, C. Castellano, P. Van Mieghem, and A. Vespignani, Reviews of modern physics **87**, 925 (2015).
 - [6] H. W. Hethcote, SIAM review **42**, 599 (2000).
 - [7] M. Granovetter, American Journal of Sociology **83**, 1420 (1978).
 - [8] E. Bakshy, J. M. Hofman, W. A. Mason, and D. J. Watts, in *Proceedings of the Fourth ACM International Conference on Web Search and Data Mining* (ACM, 2011) pp. 65–74.
 - [9] S. Pei, L. Muchnik, J. S. Andrade Jr, Z. Zheng, and H. A. Makse, Scientific reports **4**, 5547 (2014).
 - [10] Z.-K. Zhang, C. Liu, X.-X. Zhan, X. Lu, C.-X. Zhang, and Y.-C. Zhang, Physics Reports **651**, 1 (2016).
 - [11] N. E. Friedkin and F. Bullo, Proceedings of the National Academy of Sciences **114**, 11380 (2017).
 - [12] K. T. Eames and M. J. Keeling, Proceedings of the National Academy of Sciences **99**, 13330 (2002).
 - [13] D. Kempe, J. Kleinberg, and É. Tardos, in *Proceedings of the ninth ACM SIGKDD international conference on Knowledge discovery and data mining* (ACM, 2003) pp. 137–146.
 - [14] C. Kiss and M. Bichler, Decision Support Systems **46**, 233 (2008).
 - [15] L. Lü, D. Chen, X.-L. Ren, Q.-M. Zhang, Y.-C. Zhang, and T. Zhou, Physics Reports **650**, 1 (2016).
 - [16] A. Galeotti and S. Goyal, The RAND Journal of Economics **40**, 509 (2009).
 - [17] O. Hinz, B. Skiera, C. Barrot, and J. U. Becker, Journal of Marketing **75**, 55 (2011).
 - [18] D. J. Watts and P. S. Dodds, Journal of consumer research **34**, 441 (2007).
 - [19] R. Iyengar, C. Van den Bulte, and T. W. Valente, Marketing Science **30**, 195 (2011).
 - [20] P. Domingos and M. Richardson, in *Proceedings of the seventh ACM SIGKDD international conference on Knowledge discovery and data mining* (ACM, 2001) pp. 57–66.
 - [21] J. Leskovec, L. A. Adamic, and B. A. Huberman, ACM Transactions on the Web (TWEB) **1**, 5 (2007).
 - [22] R. Cohen, S. Havlin, and D. Ben-Avraham, Physical Review Letters **91**, 247901 (2003).
 - [23] J. Borge-Holthoefer and Y. Moreno, Physical Review E **85**, 026116 (2012).
 - [24] M. Kitsak, L. K. Gallos, S. Havlin, F. Liljeros, L. Muchnik, H. E. Stanley, and H. A. Makse, Nature physics **6**, 888 (2010).
 - [25] G. F. de Arruda, A. L. Barbieri, P. M. Rodríguez, F. A. Rodrigues, Y. Moreno, and L. da Fontoura Costa, Physical Review E **90**, 032812 (2014).
 - [26] F. Bauer and J. T. Lizier, EPL (Europhysics Letters) **99**, 68007 (2012).
 - [27] F. Radicchi and C. Castellano, Physical Review E **93**, 062314 (2016).
 - [28] A.-L. Barabási, *Network science* (Cambridge University Press, 2016).
 - [29] H. Liao, M. S. Mariani, M. Medo, Y.-C. Zhang, and M.-Y. Zhou, Physics Reports **689**, 1 (2017).
 - [30] L. Katz, Psychometrika **18**, 39 (1953).
 - [31] D. Chen, L. Lü, M.-S. Shang, Y.-C. Zhang, and T. Zhou, Physica a: Statistical mechanics and its applications **391**, 1777 (2012).
 - [32] A. Zeng and C.-J. Zhang, Physics Letters A **377**, 1031 (2013).
 - [33] J.-G. Liu, Z.-M. Ren, and Q. Guo, Physica A: Statistical Mechanics and its Applications **392**, 4154 (2013).
 - [34] L. Lü, T. Zhou, Q.-M. Zhang, and H. E. Stanley, Nature communications **7**, 10168 (2016).
 - [35] R. Pastor-Satorras and C. Castellano, Physical Review E **95**, 022301 (2017).
 - [36] G. Lawyer, Scientific reports **5**, 8665 (2015).
 - [37] P. Bonacich, Journal of Mathematical Sociology **2**, 113 (1972).
 - [38] F. Iannelli, A. Koher, D. Brockmann, P. Hövel, and I. M. Sokolov, Phys. Rev. E **95**, 012313 (2017).
 - [39] N. E. Friedkin, P. Jia, and F. Bullo, Sociological Science **3**, 444 (2016).
 - [40] S. Brin and L. Page, Computer networks and ISDN systems **30**, 107 (1998).
 - [41] D. J. Watts and S. H. Strogatz, nature **393**, 440 (1998).
 - [42] R. Pastor-Satorras and A. Vespignani, Physical review letters **86**, 3200 (2001).
 - [43] D. J. Watts, Proceedings of the National Academy of Sciences **99**, 5766 (2002).
 - [44] D. Brockmann and D. Helbing, Science **342**, 1337 (2013).
 - [45] We assume that the network is connected.
 - [46] To compare ViralRank’s performance with that of metrics that rank the nodes in order of *decreasing* score (e.g., degree), we use $-v$ in Figs. 3, 4 and 5. In this way, the nodes are again ranked in order of decreasing (yet increasing in modulus) score. To keep the terminology simple, we always refer to the correlation between $-v$ and node’s spreading ability as ViralRank’s performance.
 - [47] This MFPT is also known as global MFPT [74].
 - [48] D. Gleich, SIAM Review **57**, 321 (2015).
 - [49] T. Martin, X. Zhang, and M. Newman, Physical review E **90**, 052808 (2014).
 - [50] The epidemic threshold for the SIR model can be estimated within the degree-block approximation, i.e. assuming no degree correlations, as [75] $\beta_c = \langle k \rangle / (\langle k^2 \rangle - \langle k \rangle)$, where $k_i = \sum_j A_{ij}$ denotes the degree.

- [51] D. Balcan, B. Gonçalves, H. Hu, J. J. Ramasco, V. Colizza, and A. Vespignani, *Journal of computational science* **1**, 132 (2010).
- [52] P. Bajardi, C. Poletto, J. J. Ramasco, M. Tizzoni, V. Colizza, and A. Vespignani, *PloS one* **6**, e16591 (2011).
- [53] W. Van den Broeck, C. Gioannini, B. Gonçalves, M. Quagiotto, V. Colizza, and A. Vespignani, *BMC infectious diseases* **11**, 37 (2011).
- [54] M. Tizzoni, P. Bajardi, C. Poletto, J. J. Ramasco, D. Balcan, B. Gonçalves, N. Perra, V. Colizza, and A. Vespignani, *BMC medicine* **10**, 165 (2012).
- [55] V. Colizza, A. Barrat, M. Barthélemy, and A. Vespignani, *BMC Medicine* **5**, 1 (2007).
- [56] V. Colizza, A. Barrat, M. Barthélemy, and A. Vespignani, *Proceedings of the National Academy of Sciences of the United States of America* **103**, 2015 (2006).
- [57] M. Rosvall, A. V. Esquivel, A. Lancichinetti, J. D. West, and R. Lambiotte, *Nature Communications* **5** (2014).
- [58] I. Scholtes, N. Wider, R. Pfitzner, A. Garas, C. J. Tessone, and F. Schweitzer, *Nature Communications* **5**, 5024 EP (2014).
- [59] P. Holme, *Physical Review E* **94**, 022305 (2016).
- [60] F. Morone and H. A. Makse, *Nature* **524**, 65 (2015).
- [61] V. E. Krebs, *Connections* **24**, 43 (2002).
- [62] R. Michalski, S. Palus, and P. Kazienko, “Matching organizational structure and social network extracted from email communication,” in *Business Information Systems: 14th International Conference, BIS 2011, Poznań, Poland, June 15-17, 2011. Proceedings*, edited by W. Abramowicz (Springer Berlin Heidelberg, Berlin, Heidelberg, 2011) pp. 97–206.
- [63] P. M. Gleiser and L. Danon, *Advances in complex systems* **6**, 565 (2003).
- [64] M. E. Newman, *Physical review E* **74**, 036104 (2006).
- [65] S. Coulomb, M. Bauer, D. Bernard, and M.-C. Marsolier-Kergoat, *Proceedings of the Royal Society B: Biological Sciences* **272**, 1721 (2005).
- [66] J. Leskovec and J. J. Mcauley, in *Advances in neural information processing systems* (2012) pp. 539–547.
- [67] V. Colizza, R. Pastor-Satorras, and A. Vespignani, *Nature Physics* **3**, 276 (2007).
- [68] J. R. Norris, *Markov Chains* (Cambridge University Press, 1998).
- [69] J. G. Kemeny and J. L. Snell, (1960).
- [70] G. Parisi, *Statistical Field Theory* (Addison-Wesley Pub. Co., 1988).
- [71] N. E. Friedkin, *American Journal of Sociology* **96**, 1478 (1991).
- [72] N. E. Friedkin and E. C. Johnsen, *Social Networks* **39**, 12 (2014).
- [73] R. Lambiotte and M. Rosvall, *Physical Review E* **85**, 056107 (2012).
- [74] V. Tejedor, O. Bénichou, and R. Voituriez, *Physical Review E* **80**, 065104 (2009).
- [75] A. Barrat, M. Barthélemy, and A. Vespignani, *Dynamical Processes on Complex Networks* (Cambridge University Press, 2008).
- [76] K.-i. Hashimoto, *Automorphic forms and geometry of arithmetic varieties.* , 211 (1989).
- [77] F. Krzakala, C. Moore, E. Mossel, J. Neeman, A. Sly, L. Zdeborová, and P. Zhang, *Proceedings of the National Academy of Sciences* **110**, 20935 (2013).
- [78] B. A. N. Travençolo and L. d. F. Costa, *Physics Letters A* **373**, 89 (2008).
- [79] J. L. Aron, M. O’leary, R. A. Gove, S. Azadegan, and M. C. Schneider, *Computers & Security* **21**, 142 (2002).
- [80] R. M. Anderson, R. M. May, and B. Anderson, *Infectious diseases of humans: dynamics and control*, Vol. 28 (Wiley Online Library, 1992).
- [81] L. Meyers, *Bulletin of the American Mathematical Society* **44**, 63 (2007).
- [82] J. O. Kephart, S. R. White, and D. M. Chess, *IEEE Spectrum* **30**, 20 (1993).
- [83] J. O. Kephart, G. B. Sorkin, D. M. Chess, and S. R. White, *Scientific American* **277**, 88 (1997).
- [84] The normalization of g_i also implies that π_i is normalized to unity.
- [85] This condition is always satisfied by definition of effective distance.
- [86] W. W. Zachary, *Journal of anthropological research* **33**, 452 (1977).
- [87] D. Lusseau, K. Schneider, O. J. Boisseau, P. Haase, E. Slooten, and S. M. Dawson, *Behavioral Ecology and Sociobiology* **54**, 396 (2003).
- [88] D. E. Knuth, *The Stanford GraphBase: a platform for combinatorial computing*, Vol. 37 (Addison-Wesley Reading, 1993).